Inorganic Chemistry

ARTICLE

pubs.acs.org/IC

Mechanistic Insight into Protonolysis and Cis−Trans Isomerization of Benzylplatinum(II) Complexes Assisted by Weak Ligand-to-Metal Interactions. A Combined Kinetic and DFT Study†

Emanuela Guido,[‡] Giuseppina D'Amico,[‡] Nino Russo,[§] Emilia Sicilia,[§] Silvia Rizzato,[⊥] Alberto Albinati,[⊥] Andrea Romeo,[‡] M. Rosaria Plutino,*[,¶] and Raffaello Romeo[‡]

[‡]Dipartimento di Chimica Inorganica, Chimica Analitica e Chimica Fisica, Università di Messina, Viale F. Stagno D'Alcontres 31, Vill. S. Agata, I-98166 Messina, Italy

[§]Dipartimento di Chimica, Università della Calabria, I-87030 Arcavacata di Rende (Cs), Italy

[⊥]Dipartimento di Chimica Strutturale e Facoltà di Farmacia, via Venezian 21, Università di Milano, Milano, Italy

[¶]Istituto per lo Studio dei Materiali Nanostrutturati, ISMN-CNR, Unità di Messina-Sezione di Palermo, c/o Dip. di Chim. Inorg., Chim. Anal., Chim. Fis., Università di Messina, Viale F. Stagno D'Alcontres 31, Vill. S. Agata, I-98166 Messina, Italy

Supporting Information

ABSTRACT: Low-temperature NMR measurements showed that protonolysis and deuterolysis by H(D)X acids on meta- and para-substituted dibenzylplatinum(II) complexes *cis*-[Pt-$(CH_2Ar)_2(PEt_3)_2$] (Ar = $C_6H_4Y^-$; Y = 4-Me, **1a**; 3-Me, **1b**; H, **1c**; 4-F, **1d**; 3-F, **1e**; 4-Cl, **1f**; 3-Cl, **1g**; 3-CF_3, **1h**) in CD_3OD leads directly to the formation of *trans*-$[Pt(CH_2Ar)(PEt_3)_2$-$(CD_3OD)]X$ (**4a**−**4h**) and toluene derivatives. The reaction obeys the rate law $k_{obsd} = k_H[H^+]$. For $CH_2Ar = CH_2C_6H_5^-$, $k_H = 176 \pm 3\ M^{-1}\ s^{-1}$ and $k_D = 185 \pm 5\ M^{-1}\ s^{-1}$ at 298.2 K, $\Delta H^{\ddagger} = 46 \pm 1\ kJ\ mol^{-1}$ and $\Delta S^{\ddagger} = -47 \pm 1\ J\ K^{-1}\ mol^{-1}$. In contrast, in acetonitrile-d_3, three subsequent stages can be distinguished, at different temperature ranges: (i) instantaneous formation of new benzylhydridoplatinum(IV) complexes *cis*-$[Pt(CH_2Ar)_2(H)(CD_3CN)(PEt_3)_2]X$ (**2a**−**2h**, at 230 K), (ii) reductive elimination of **2a**−**2h** to yield *cis*-$[Pt(CH_2Ar)(CD_3CN)(PEt_3)_2]X$ (**3a**−**3h**) and toluene derivatives (in the range 230−255 K), and finally (iii) spontaneous isomerization of the cis cationic solvento species to the corresponding trans isomers (**4a**−**4h**, in the range 260−280 K). All compounds were detected and fully characterized through their ^1H and $^{31}P\{^1H\}$ NMR spectra. Kinetics monitored by ^1H and $^{31}P\{^1H\}$ NMR and isotopic scrambling experiments on *cis*-$[Pt(CH_2Ar)_2(H)(CD_3CN)(PEt_3)_2]X$ gave some insight onto the mechanism of reductive elimination of **2a**−**2h**. Systematic kinetics of isomerization of **3a**−**3h** were followed in the temperature range 285−320 K by stopped-flow techniques. The process goes, as expected, through the relatively slow dissociative loss of the weakly bonded solvent molecule and interconversion of two geometrically distinct T-shaped three-coordinate intermediates. The dissociation energy depends upon the solvent-coordinating ability. DFT optimization reveals that along the energy profile the "cis-like" $[Pt(CH_2Ar)(PMe_3)_2]^+$ intermediate is strongly stabilized by a Pt···η^2-C1−C_{ipso} bond between the unsaturated metal and benzyl carbons. The value of the ensuing stabilization energy was estimated by computational data to be greater than that found for similar β-agostic Pt···η^2-CH interactions with alkyl groups containing β-hydrogens. An observed consequence of the strong stabilization of "*cis*"-$[Pt(\eta^2\text{-}CH_2Ar)(PMe_3)_2]^+$ is the remarkable acceleration of the rate of isomerization, greater than that produced by the so-called "β-hydrogen kinetic effect". Kinetic and DFT data concur to indicate that electron donation by substituents on the benzyl ring leads to further stabilization of the "*cis*"-$[Pt(\eta^2\text{-}CH_2Ar)(PMe_3)_2]^+$ cationic species.

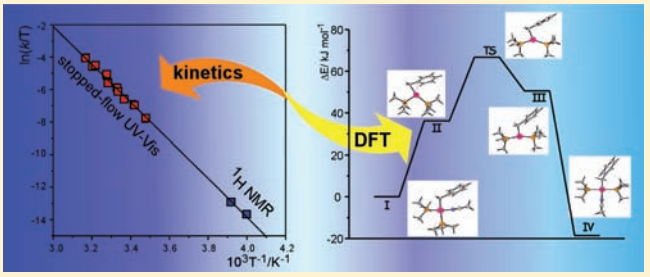

INTRODUCTION

For many years[1] "14-electron", T-shaped, three-coordinate intermediates, formed upon ligand dissociation from d^8 square-planar organometallic complexes, have been cursorily depicted in catalytic cycles, bond activation reactions, substitution reactions, geometrical isomerizations, transmetalations, etc. In particular, such coordinatively and electronically unsaturated species play a vital role as key intermediates in many catalytic transformations of organic substrates. Looking at the literature data, it is possible to see that very often the presence of such compounds as elusive and transient species has been inferred simply from the observation of mass-law retardation effects. A more complicated protocol involving the measurement and rationalization of a multiplicity of kinetic effects (rates of ligand exchange and substitution, saturation plots, electronic, steric, solvent, and isotopic effects, activation parameters, etc.) has been rarely applied. Whatever the degree of sophistication of the kinetic approach is, direct proof of the existence of three-coordinate,

Received: September 13, 2010
Published: February 22, 2011

   dx.doi.org/10.1021/ic101879s | *Inorg. Chem.* 2011, 50, 2224–2239

Chart 1. Variety of Metal−Benzyl Linkages

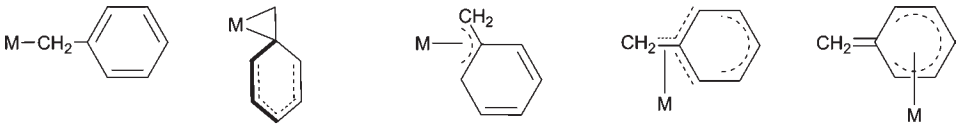

η^1 η^2 η^3 η^4 η^5

14-electron compounds in solution is difficult to find. Because of the exceptionally high Lewis acidity inherent in these 14-electron metal complexes, they tend to interact with even the weakest of nucleophiles, and the empty coordination sites can be filled by counterions or by even very weakly coordinating solvent molecules.[2] The formation of dimers could also well be a reasonable alternative.[3] Recent reports on the isolation and structural characterization of a few three-coordinate, T-shaped rhodium(I),[4] cobalt(I),[5] nickel(II),[6] palladium(II),[7] and platinum(II)[8] compounds have fortunately helped to have an insight into the structural and bonding characteristics of such compounds that appear to be stabilized by auxiliary bonding interactions. One of the oldest examples of this kind concerns the cation $Rh(PPh_3)_3^+$, which achieves a 16-electron as a consequence of interaction with a C=C bond of a dangling phenyl group.[3b] Other examples can be found in the literature in which the immediately adjacent double bond of a PPh_3 donor or a variety of remote olefins is involved in bonding with the metal.[9] The large majority of the isolated three-coordinate d^8 ML_3 species show C−H bonds involved in agostic interactions to the empty coordination site of otherwise 14-electron, T-shaped d^8 complexes. In platinum(II) chemistry, these examples include the cationic $[Pt(R)(P{-}P)]^+$ complexes (P−P = chelating ligand; R = ethyl, norbornyl),[8a,8b] the very recent $[Pt(CH_3)(^tPr_3P)_2]^+$,[8c] and the novel "T-shaped, 14-electron" platinum(II) cations *trans*-$[Pt(CH_3)L_2]^+$ [L = PR_2(2,6-$Me_2C_6H_3$); R = Ph, Cy].[8d] However, no notable C−H agostic interaction with the metal center was detected in a series of cationic T-shaped boryl complexes of the type *trans*-$\{(Cy_3P)_2Pt[B(X)X']\}^+$,[8e,8f] in a series of palladium(II) complexes $[PdArXL]$[7c] (Ar = aryl group; X= amido group; L= phosphane), and in the rhodium(I) complex $[Rh(NNN)]BArF$.[4e] Unprecedented examples of bare 14-electron planar four-coordinate d^6 RhL_4 and d^6 IrL_4 metal complexes have been reported by Nolan et al.[10] π donation, from a lone pair on a donor atom already bound to the metal (e.g., $R_2N{-}M$), is crucial in understanding the remarkable stability as well as the lack of agostic interactions in the 14-electron compounds.[10,8e,3a]

Thus, the challenge to isolate "14-electron", T-shaped compounds seems to rely on the use of ligands that guarantee some form of protection of the fourth-coordination site and of electron transfer to the vacant σ orbital of the metal. To what extent such electron transfer occurs is a matter of debate.[2] However, when occurring within a transition state (TS) or a reaction intermediate, agostic or "preagostic" interactions are shown to produce the so-called "β-hydrogen kinetic effect", a sharp acceleration of the reaction rate.[11] The combined kinetic and density functional theory (DFT) study of the uncatalyzed isomerization of cationic solvent complexes of the type *cis*-$[Pt(R')(S)(PR_3)_2]^+$ to their trans isomers, perhaps the best-documented example[12] of a process driven by ligand dissociation in platinum(II) chemistry,[13] has shown that when R′ is a linear alkyl the "cis-like" three-coordinate $[Pt(R')(PEt_3)_2]^+$ reaction intermediate was stabilized by a classical Pt−η^2-CH agostic interaction with the electron pair of a hanging C−H bond. The bond energy was estimated by both kinetic and computational data to be in the range of 21−33 kJ mol^{-1}. The structure and bonding features of *cis*-$[Pt(R')(PMe_3)_2]^+$ have been discussed in detail and have been taken as a model of the first approach of a C−H bond to an unsaturated metal center prior to C−H activation.

In searching for similar effects, we were prompted to analyze the behavior of benzyl complexes because it is known that the benzyl ligand differs from simple alkyl groups in its capability of adopting a variety of metal−benzyl linkages ranging from the classical η^1 bonding to the rather unusual η^5 bonding (Chart 1).

All of these structural types have been reported in the literature and, in some cases, authenticated by X-ray crystallography.[14] A relevant feature of the present work is the discovery of the formation of an η^2-Pt−C1−C_{ipso} bond within the transient intermediate of formula $[Pt(\eta^2\text{-}CH_2C_6H_5)(PMe_3)_2]^+$, which is somewhat stronger than that found for the agostic $[Pt(\eta^2\text{-}CH_2CH_3)(PR_3)_2]^+$ species. This strong stabilization is at the origin of a marked rate acceleration. Tuning the energy of reaction intermediates can be a powerful mechanistic tool in the control of organometallic reactions, especially those involving bond activation.

RESULTS

Synthesis and Characterization of the Complexes. All the dibenzyl complexes *cis*-$[Pt(CH_2Ar)_2(PEt_3)_2]$ (Ar = $C_6H_4Y^-$; Y = 4-Me, **1a**; 3-Me, **1b**; H, **1c**; 4-F, **1d**; 3-F, **1e**; 4-Cl, **1f**; 3-Cl, **1g**; 3-CF_3, **1h**; shown in Chart 2) were synthesized from the reaction of *cis*-$[PtCl_2(PEt_3)_2]$ with benzylmagnesium halides following essentially the synthetic procedure described by Chatt and Shaw for compound **1c**.[15] The desired products were obtained as solids in high yield and purity and were characterized by elemental analysis and ^1H and $^{31}P\{^1H\}$ NMR spectroscopy. The spectral characteristics of these compounds do not differ much from those of other dialkyl complexes.[16] In the ^1H NMR spectra, the phosphorus-coupled methylene resonance appears as an apparent triplet ($^3J_{PH} \approx 17$ Hz) due to virtual coupling. The $^{31}P\{^1H\}$ NMR spectra show a single resonance and low values of $^1J_{PtP}$ ($\approx$1850 Hz) that are diagnostic for a cis stereochemistry, with the phosphane ligands trans to the benzyl groups.[17] Selected NMR data for complexes **1a**−**1h** are reported in Table 1. A complete list and assignments of the NMR data are given in the Experimental Section.

Solid-State Structures of the Complexes *cis*-$[Pt(CH_2C_6H_5\text{-}4\text{-}Me)_2(PEt_3)_2]$ (1a) and *cis*-$[Pt(CH_2C_6H_5\text{-}4\text{-}Cl)_2(PEt_3)_2]$ (1f). Table 2 lists selected bond distances and angles of the platinum(II) species **1a**, and an ORTEP view of the molecule is given in Figure 1. The immediate coordination sphere around the Pt center consists of the two η^1-bonded benzyl groups, cis to each other, and the P atoms of the phosphane moieties. The Pt atom lies on a crystallographic symmetry element so that only half of the molecule is independent. The benzyl groups are on opposite sides of the coordination plane with the same orientation, imposed by symmetry, with a value of the C1′−Pt−C1−C2

dx.doi.org/10.1021/ic101879s |*Inorg. Chem.* 2011, 50, 2224–2239

Chart 2. Structural Formula for the Platinum(II) Complexes 1a−1h, 2a−2h, 3a−3h, and 4a−4h

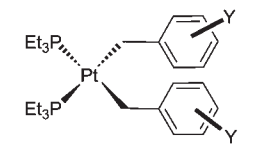

Y = *4*-Me, **1a**
3-Me, **1b**
H, **1c**
4-F, **1d**
3-F, **1e**
4-Cl, **1f**
3-Cl, **1g**
3-CF_3, **1h**

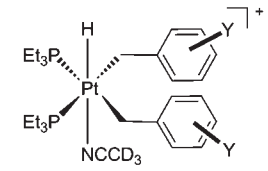

Y = *4*-Me, **2a**
3-Me, **2b**
H, **2c**
4-F, **2d**
3-F, **2e**
4-Cl, **2f**
3-Cl, **2g**
3-CF_3, **2h**

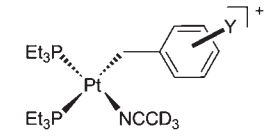

Y = *4*-Me, **3a**
3-Me, **3b**
H, **3c**
4-F, **3d**
3-F, **3e**
4-Cl, **3f**
3-Cl, **3g**
3-CF_3, **3h**

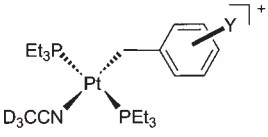

Y = *4*-Me, **4a**
3-Me, **4b**
H, **4c**
4-F, **4d**
3-F, **4e**
4-Cl, **4f**
3-Cl, **4g**
3-CF_3, **4h**

dihedral angle of 71.1(2)°. The *ipso*-C atoms of the aryl rings, closest to the Pt center, are at a distance of ca. 3.5 Å. The Pt−C and Pt−P bond lengths of 2.127(2) and 2.2945(8) Å, respectively, are unexceptional. As for the corresponding dibutyl complex,[11] the Pt−P separations are in the upper range of the values found for other phosphanedialkyl complexes of platinum(II) as a result of the strong trans influence of the carbon ligand.

An ORTEP view of compound **1f** is given in Figure 2, while selected bond distances and angles are listed in Table 2. As for **1a**, the immediate coordination sphere around the Pt center consists of two η^1-bonded benzyl groups, cis to each other, and the P atoms of the phosphane moieties. The benzyl groups lie on opposite sides of the coordination plane with slightly different orientations compared to compound **1a**, as can be judged from the values of the torsion angles (see Table 2), a difference due to the absence of symmetry constraints. Moreover, we note that the orientation of the C2 aryl ring is such that the H atom bonded to the *ipso*-carbon C7 points toward the Pt center at a distance of 2.83(1) Å in a pseudoapical position, suggesting a weak nonconventional M···H interaction (see Figure S1 in the Supporting Information).[18]

The two Pt−P and Pt−C distances are equal and comparable to those found in **1a**.

The similar values of the Pt−C and Pt−P separations and the absence of significant deformations in the bond angles for **1a**, **1f**, and *cis*-$[Pt(^nBu)_2(PEt_3)_2]$[11] indicate that the presence of an aryl ring (even with para-substituent groups) does not affect significantly the molecular structure that is comparable to that of an alkyl compound (cf. Table 2).

Table 1. Selected ^1H and $^{31}P\{^1H\}$ NMR Data for Starting *cis*-$[Pt^{II}(CH_2Ar)_2(PEt_3)_2]$ (1a−1h) Complexes and the Corresponding Benzylhydridoplatinum(IV) Species *cis*-$[Pt^{IV}(H)(CD_3CN)(CH_2Ar)_2(PEt_3)_2]X$ (2a−2h) Obtained by Oxidative Addition with HX

		cis-$[Pt^{II}(CH_2Ar)_2(PEt_3)_2]$[a]			
		^1H NMR		^{31}P NMR	
no.	Ar	$\delta(Pt-CH_2)$	$^2J_{PtH}$	δ	$^1J_{PtP}$
1a[b]	4-MeC_6H_4	2.39	83.4	12.5	1943
1b[c]	3-MeC_6H_4	2.21	83.8	12.5	1961
1c[b]	C_6H_5	2.46	83.7	12.4	1963
1d[c]	4-FC_6H_4	2.21	82.4	12.4	1954
1e[c]	3-FC_6H_4	2.17	84.6	12.4	2012
1f[c]	4-ClC_6H_4	2.20	83.8	12.5	1988
1g[c]	3-ClC_6H_4	2.39	83.1	12.6	2004
1h[c]	3-$CF_3C_6H_4$	2.44	82.5	12.8	2008

		cis-$[Pt^{IV}(H)(CD_3CN)(CH_2Ar)_2(PEt_3)_2]X$[d]					
		^1H NMR				^{31}P NMR	
no.	Ar	$\delta(Pt-H)$	$^1J_{PtH}$	$\delta(Pt-CH_2)$	$^2J_{PtH}$	δ	$^1J_{PtP}$
2a[b]	4-MeC_6H_4	−21.4	1271	2.35	65.5	−3.5	1188
2b[c]	3-MeC_6H_4					−3.5	1192
2c[b]	C_6H_5	−21.7	1253	2.30	53.6	−3.4	1198
2d[c]	4-FC_6H_4	−21.5	1260	2.25	56.6	−3.6	1200
2e[c]	3-FC_6H_4	−21.5	1256	2.28	53.6	−3.4	1216
2f[c]	4-ClC_6H_4	−21.5	1256	2.25	59.5	−3.3	1210
2g[c]	3-ClC_6H_4	−21.5	1253	2.25	65.5	−3.2	1218
2h[c]	3-$CF_3C_6H_4$					−3.4	1205

[a] In acetonitrile-d_3 at 298 K. [b] X = BArF. [c] X = OTf. [d] In acetonitrile-d_3 at 238 K.

Table 2. Selected Bond Distances (Å) and Angles (deg) for Compounds 1a[a] and 1f

	1a	**1f**
Pt−C1	2.127(2)	2.123(6)
Pt−C8	2.127(2)	2.110(6)
Pt−P1	2.2945(8)	2.297(2)
Pt−P2	2.2945(8)	2.301(2)
P1−Pt−C1	164.26(7)	173.4(2)
P2−Pt−C8	164.26(7)	166.2(2)
P1−Pt−P2	104.66(5)	99.78(6)
P1−Pt−C8	87.19(8)	91.2(2)
P2−Pt−C1	87.19(8)	86.3(2)
C1−Pt−C8	83.3(2)	83.2(3)
C1−Pt−C8−C9	−71.1(2)	−96.5
C8−Pt−C1−C2	−71.1(2)	−87.4(5)
Pt−C1−C2−C7	58.3(2)	13.1(3)
Pt−C8−C9−C14	58.3(2)	41.7(4)

[a] The numbering scheme is based on the less symmetric compound **1f** for easier comparison. The symmetry-related values in **1a** appear as double entries.

Acidolysis of Dibenzyl Complexes in Methanol. Upon the addition of a sufficient amount of an ethereal solution of HBF_4 to a solution of the platinum complex in CD_3OD, there is an immediate and sharp change of the NMR spectrum. Cleavage of the Pt−C(benzyl) σ bond takes place according to the reaction

$$cis\text{-}[Pt(CH_2Ar)_2L_2] \xrightarrow[CD_3OD]{H^+} trans\text{-}[Pt(CH_2Ar)(CD_3OD)L_2]^+ + CH_3Ar \quad (1)$$

The final trans product can be recognized particularly through the single $^{31}P\{^1H\}$ resonance due to 2 equiv of phosphane ligands. Attempts to detect by NMR at low temperature (230 K)

dx.doi.org/10.1021/ic101879s |*Inorg. Chem.* 2011, 50, 2224–2239

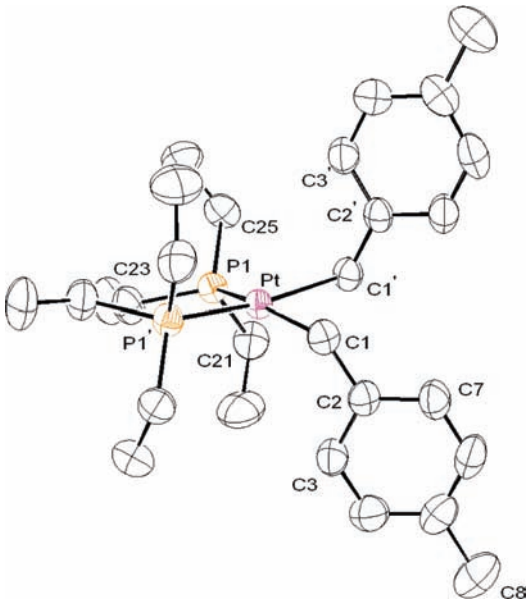

Figure 1. ORTEP view of a molecule of compound **1a** showing 50% probability ellipsoids. Primed atoms are obtained from those unprimed by the symmetry operation $-x-1, y, -z+{}^{3}/_{2}$.

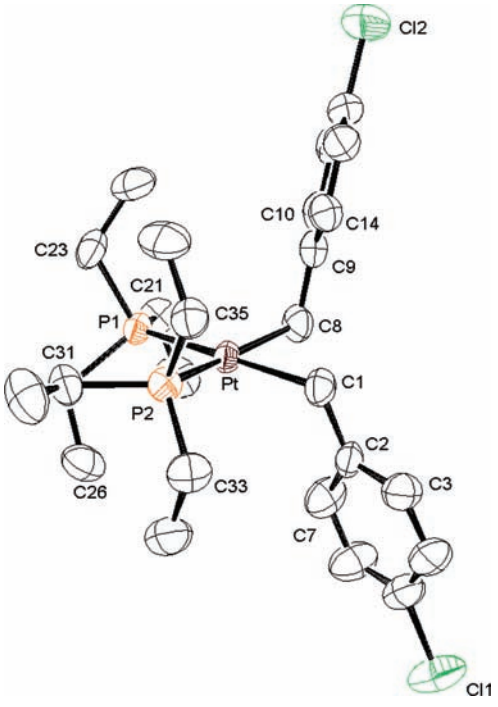

Figure 2. ORTEP view of a molecule of compound **1f** showing 50% probability ellipsoids.

the presence of the cis derivative or of possible alkylhydridoplatinum(IV) intermediates were unsuccessful. Subsequent spectrophotometric studies confirmed that the rate of cis−trans isomerization of the cationic solvento species *cis*-$[Pt(PEt_3)_2(CH_2R)(CD_3OD)]^+$ is too high to be followed even by rapid scanning spectrophotometric techniques.[19] At relatively low acid concentrations, the reaction in eq 1 went to completion in a single stage and excellent fits were obtained from regression analysis of the absorbance versus time data. The dependence of the pseudo-first-order rate constants k_{obsd} on the proton concentration (Table S1 in the Supporting Information) in methanol at 297 K is described by a straight line with zero intercept, i.e., $k_{obsd} = k_H[H^+]$. The same pattern of behavior is observed when the kinetic runs are carried out with DOTf in CH_3OD (Table S1 in the Supporting Information), i.e., $k_{obsd} = k_D[D^+]$. The values of $k_H = 176 \pm 3$ M^{-1} s^{-1} and $k_D = 185 \pm 5$ M^{-1} s^{-1} were obtained from linear regression analysis of the kinetic data. The values of k_H at different temperatures are set forth also in Table S1 in the Supporting Information, and the calculated activation parameters were $\Delta H^{\ddagger} = 46 \pm 1$ kJ mol^{-1} and $\Delta S^{\ddagger} = -47 \pm 1$ J K^{-1} mol^{-1}.

Acidolysis of Dibenzyl Complexes in Acetonitrile-d_3: Formation of Benzylhydridoplatinum(IV) Complexes. The addition of acid (HOTf, HBArF, or $HBF_4 \cdot Et_2O$) to **1a**−**1h** at low temperature in acetonitrile-d_3, according to the procedure described in the experimental part, was expected to lead to cationic solvento species *cis*- or *trans*-$[Pt(CH_2C_6H_4Y)(CH_3CN)(PEt_3)_2]^+$ and toluene derivative liberation, as described above in methanol or found before in a series of alkylphosphane complexes of the type *cis*-$[PtMe_2L_2]$, *cis*-$[PtMe_2(L-L)]$, and *cis*-$[PtMeClL_2]$.[16] In contrast, at 230 K, the $^{31}P\{^1H\}$ NMR spectra showed a single upfield resonance with values of $^1J_{PtP}$ (≈1200 Hz) much lower than those of the precursors **1a**−**1h** (≈1980 Hz). A characteristic Pt−H resonance appears far upfield in the ^1H NMR spectra ($\delta \sim -21$ ppm) with the corresponding platinum satellites ($^1J_{PtH} \sim 1250$ Hz), the Pt−CH_2R resonance remains almost unchanged with respect to that of **1a**−**1h** ($\delta \sim 2.30$ ppm), showing a lower value of the ^{195}Pt satellite signal ($^2J_{PtH} \approx 60$ Hz), and the ethyl groups of the phosphanes show the typical splitting patterns of a triplet ($\delta \sim 0.80$ ppm) and a quartet ($\delta \sim 1.60$ ppm), each integrating for 18 and 12 protons, respectively. There was no evidence for the buildup of toluene derivatives in solution. All these findings indicate that the addition of HX to the planar **1a**−**1h** substrates generates rather stable benzylhydridoplatinum(IV) complexes according to the reaction

$$cis\text{-}[Pt(CH_2Ar)_2L_2] \xrightarrow[CD_3CN]{H^+} cis\text{-}[Pt(CH_2Ar)_2(H)(CD_3CN)L_2]^+ \quad (2)$$

The ^1H and ^{31}P NMR resonances of the hydride compounds **2a**−**2h** showed no significant changes upon a change in the nature of the acid used (HOTf, HBF_4, HBArF, or even HCl) so that we can safely conclude that the sixth-coordinated group is a molecule of acetonitrile, which concurs to confer particular stability to the octahedral species. The magnitudes of the coupling constants $^1J_{PtP}$ are consistent with a stereochemical arrangement in which H and CD_3CN reside trans each other, for example, in the apical positions of the octahedral structure, while phosphanes and benzyl groups maintain their original position in the equatorial plane resembling the starting square-planar arrangement. The magnetic equivalence of the two benzyl moieties removes from consideration the possibility that a secondary interaction between the metal and a benzyl group, of the type discussed in the introductory part of this work, can be held responsible for the stability of an otherwise five-coordinate species. Selected NMR data for complexes **2a**−**2h** are reported in Table 1. A complete list and assignments of the NMR data are given in the Experimental Section.

Reductive Elimination of Benzylhydridoplatinum(IV) Complexes. At 230 K, acid addition to **1a**−**1h**, according to eq 2, leads to the quantitative formation of platinum(IV) hydrido compounds **2a**−**2h**. The reductive-elimination reactions of these

dx.doi.org/10.1021/ic101879s |*Inorg. Chem.* 2011, 50, 2224–2239

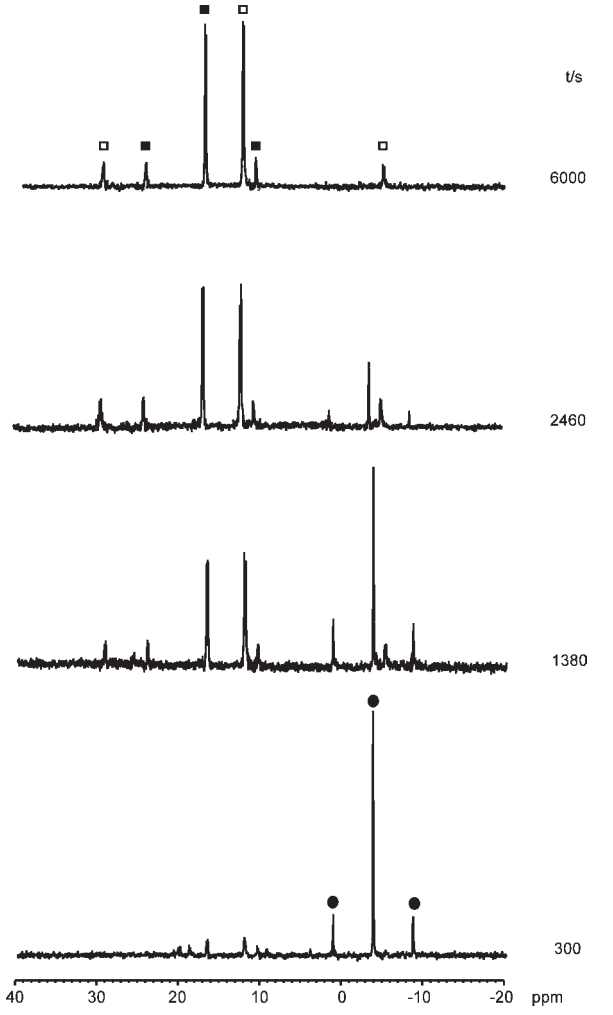

Figure 3. $^{31}P\{^1H\}$ NMR spectra (122 MHz) of **2d** (C_{Pt} = 29 mM in CD_3CN) at 238.5 K as a function of time. $^{31}P\{^1H\}$ signal of compound **2d** (δ = −3.6 ppm, $^1J_{PtP}$ = 1200 Hz); $^{31}P\{^1H\}$ signals of compound **3d** (δ = 16.7 ppm, $^1J_{PtP}$ = 1788 Hz; δ = 12.1 ppm, $^1J_{PtP}$ = 4177 Hz).

latter compounds takes place easily in acetonitrile-d_3, in the temperature range 230−255 K, according to eq 3, and can be followed by means of ^1H and ^{31}P NMR.

$$cis\text{-}[Pt(CH_2Ar)_2(H)(CD_3CN)L_2]^+ \rightarrow cis\text{-}[Pt(CH_2Ar)(CD_3CN)L_2]^+ + CH_3Ar \quad (3)$$

Taking as an example the case of compound **2d**, in Figure 3, we see that there was no evidence in the NMR spectra for the buildup of significant amounts of any other intermediate species, and only the starting platinum(IV) complex and the solventoplatinum(II) product **3d** were found in solution. The progress of the reaction can be monitored through a decrease of the intensity of the phosphorus resonance of **2d** and a parallel matching increase of the two magnetically nonequivalent phosphorus resonances of **3d**. The latter are characterized by completely different values of the coupling constant with ^{195}Pt, as a consequence of the different trans influence of the benzyl or CD_3CN ligands ($^1J_{PtP}$ = 1788 Hz for P_A, in a trans position to the C atom, and $^1J_{PtP}$ = 4177 Hz for P_B, in a trans position to CD_3CN).

The procedure adopted for **2d** was repeated for the entire set of **2a**−**2h** compounds, leaving the reactions to go to completion at a controlled low temperature (T = 231.7 K). Selected NMR data for the final complexes **3a**−**3h** are reported in Table 3. A complete list and assignments of the NMR data are given in the Experimental Section. Alternatively, the reaction can be monitored by ^1H NMR spectra, measuring the integrals of selected peaks (of the growing toluene derivative, for instance) as a function of time and using the calculated concentrations in the fitting procedure for calculation of the rate constant. The temperature dependence of the reductive-elimination reaction of **2d** was measured by both ^1H and ^{31}P NMR, as described above. Exponential curves for the change with time of the molar fraction of the reactant and of the product are illustrated in Figure S2 in the Supporting Information. The pseudo-first-order rate constants, k_{obsd}/s^{-1}, are collected in Table S2 in the Supporting Information and were fitted to the Eyring equation to yield the values of the activation parameters $\Delta H^{\ddagger}$ = 63.8 ± 3.5 kJ mol^{-1} and of $\Delta S^{\ddagger}$ = −29.0 ± 14.6 J K^{-1} mol^{-1}. The Eyring plot is

Table 3. Selected ^1H and $^{31}P\{^1H\}$ NMR Data for Cis (3a−3h) and Trans (4a−4h) Monoalkyl Cationic Solvento Complexes $[Pt(CH_2Ar)(CD_3CN)(PEt_3)_2]^+$ Obtained upon Reductive Elimination from 2a−2h and Subsequent Isomerization[a]

cis-$[Pt(CD_3CN)(CH_2Ar)(PEt_3)_2]^+$		^1H NMR		^{31}P NMR	
no.	Ar	δ(Pt−CH_2)	$^2J_{PtH}$	δ	$^1J_{PtP}$
3a	4-MeC_6H_4	2.29	60.2	16.9	1790
				12.2	4142
3b	3-MeC_6H_4	2.30	58.5	16.9	1789
				12.3	4196
3c	C_6H_5	2.33	61.8	16.9	1775
				12.2	4185
3d	4-FC_6H_4	2.31	64.8	16.7	1788
				12.1	4177
3e	3-FC_6H_4	2.33	61.8	16.7	1806
				11.7	4156
3f	4-ClC_6H_4	2.31	61.2	16.8	1797
				11.9	4168
3g	3-ClC_6H_4	2.31	61.8	16.7	1828
				11.9	4141
3h	3-$CF_3C_6H_4$	2.30	60.8	16.8	1796
				12.2	4178
trans-$[Pt(CD_3CN)(CH_2Ar)(PEt_3)_2]^+$		^1H NMR		^{31}P NMR	
no.	Ar	δ(Pt−CH_2)	$^2J_{PtH}$	δ	$^1J_{PtP}$
4a	4-MeC_6H_4	2.60	98.1	20.8	2783
4b	3-MeC_6H_4	2.44	91.2	20.8	2778
4c	C_6H_5	2.65	98.7	20.7	2769
4d	4-FC_6H_4	2.61	98.4	20.6	2756
4e	3-FC_6H_4	2.49	99.3	20.4	2736
4f	4-ClC_6H_4	2.63	99.3	20.5	2740
4g	3-ClC_6H_4	2.62	98.7	20.4	2730
4h	3-$CF_3C_6H_4$	2.24	99.0	20.5	2713

[a] Recorded in CH_3CN-d_3 as the solvent at 238.5 K for the cis solvento complexes and at 298 K for the trans solvento derivatives.

dx.doi.org/10.1021/ic101879s |*Inorg. Chem.* 2011, 50, 2224–2239

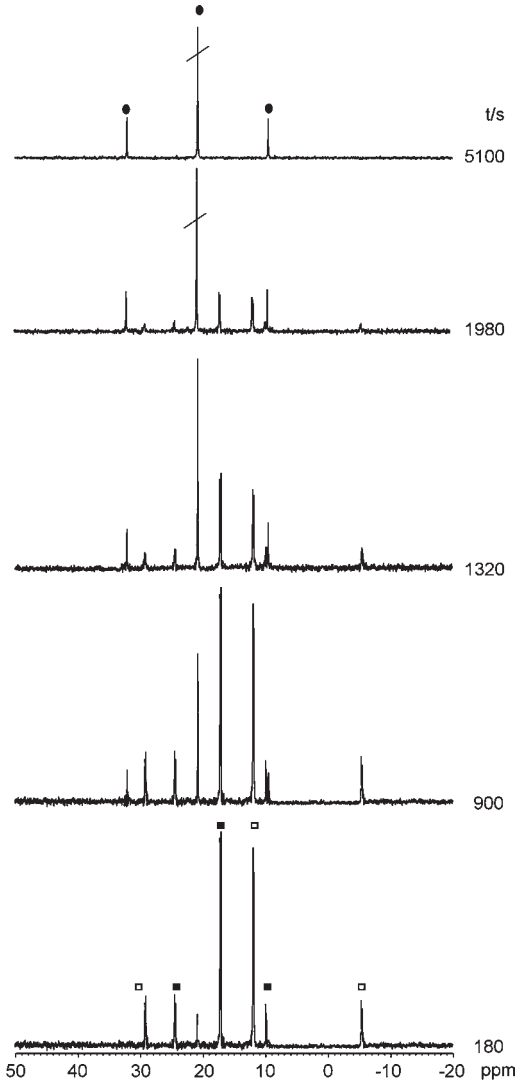

Figure 4. ^{31}P NMR spectral changes associated with the geometrical isomerization of the *cis*-solventoplatinum(II) complex **3d** to **4d** in CD_3CN at 260 K.

illustrated in Figure S3 in the Supporting Information. Kinetic measurements, carried out in CD_2Cl_2 at 233 K, in the presence of variable amounts of CD_3CN, showed that the rate of reductive elimination decreases with an increase in the CD_3CN concentration.

Geometrical Isomerization in Acetonitrile. The spontaneous geometrical isomerization of **3a**−**3h** can be monitored by NMR techniques in the temperature range 260−280 K through a decrease of the two associated ^{31}P signals and a parallel and matching increase in the signal of the corresponding trans complex, which appears as a singlet with platinum satellites (Figure 4).

Therefore, the isomerization process in acetonitrile-d_3 is described by the reaction

$$cis\text{-}[Pt(CH_2Ar)(CD_3CN)L_2]^+ \rightarrow trans\text{-}[Pt(CH_2Ar)(CD_3CN)L_2]^+ \quad (4)$$

Selected NMR data for the final reaction products **4a**−**4h** are reported in Table 3. A complete characterization and assignments of the NMR data are given in the Experimental Section.

A control, at sufficiently low temperature, by rapid scanning spectrophotometry ensured that conversion was 100% complete,

Table 4. Effect of Variation of the Nature of Ar on the Rates and Activation Parameters of the Spontaneous Isomerization of *cis*-$[Pt(CH_2Ar)(CH_3CN)(PEt_3)_2]^+$ (3a−3h) to 4a−4h in an Acetonitrile Solution

no.	Ar	k_i[a]	$\Delta H^{\ddagger}$[b]	$\Delta S^{\ddagger}$[c]	$\Delta G^{\ddagger}$[d]
3a	4-MeC_6H_4	1.83	81.8 ± 2	34 ± 5	71.6
3b	3-MeC_6H_4	1.48	89.9 ± 1	60 ± 2	72.0
3c	C_6H_5	0.820	83.8 ± 2	35 ± 4	73.4
3d	4-FC_6H_4	0.585	97.1 ± 1	76 ± 4	74.4
3e	3-FC_6H_4	0.115	104.0 ± 2	86 ± 7	78.4
3f	4-ClC_6H_4	0.159	103.4 ± 1	87 ± 3	77.1
3g	3-ClC_6H_4	0.0758	105.0 ± 4	86 ± 10	79.4
3h	3-$CF_3C_6H_4$	0.0555	95.7 ± 2	52 ± 6	80.2

[a] First-order rate constants (s^{-1}) for isomerization at 298.2 K. [b] Enthalpies of activation (kJ mol^{-1}). [c] Entropies of activation (J K^{-1} mol^{-1}). [d] Calculated free-energy of activation (kJ mol^{-1}) at 298.2K.

with spectral changes showing well-defined isosbestic points. The systematic kinetics of isomerization were followed by stopped-flow spectrophotometric techniques at fixed wavelengths, where the difference of absorbance between cis and trans compounds was largest. An example of a stopped-flow kinetic plot is illustrated in Figure S4 in the Supporting Information. The pseudo-first-order rate constants k_i for the reaction of eq 4 at various temperatures are reported in Table S3 in the Supporting Information and were analyzed by least-squares regression of linear Eyring plots. The values of k_i at 298.2 K, together with the associated activation parameters, are listed in Table 4.

Computational Data. The analyzed processes, in the framework of DFT, were the geometrical conversion of the benzylsolvento complexes *cis*-$[Pt(CH_2Ar)(S)(PMe_3)_2]^+$ (Ar = C_6H_5 and 4-ClC_6H_4; S = acetonitrile and methanol) and of *cis*-$[Pt(CH_2Ar)(CH_3CN)(PMe_3)_2]^+$ (Ar = 4-MeC_6H_4). The aim was to obtain insight into the way in which the different nature of the substituent group on the aromatic ring of the labile coordinated solvent could affect the various steps along the reaction coordinate. Geometry optimizations were performed for the initial and final complexes and for the main intermediates along the energy profile. The relevant computational data listed in Table 5 refer to the energetics of the isomerization of various species *cis*-$[Pt(CH_2Ar)(S)(PMe_3)_2]^+$ in which the nature of the benzyl group and of the leaving group has been changed. Relative energies, calculated with respect to the reactant cationic solvento complex, of the intermediates, of the TS for their conversion, and of the product state are in kilojoules per mole. Cartesian coordinates of the B3LYP-optimized, T-shaped *cis*- and *trans*-$[Pt(CH_2C_6H_4Y)(PMe_3)_2]^+$ (Y = H, 4-Cl, 4-Me) complexes are given in Table S4 in the Supporting Information.

DISCUSSION

NMR Features of Benzylhydridoplatinum(IV) Complexes. As discussed before, among the six possible stereoisomers for an octahedral species of the type Ma_2b_2cd, only one is compatible with a single ^{31}P resonance (two magnetically equivalent P atoms) and with its very low $^1J_{PtP}$ coupling constant (the presence of a couple of strong trans-activating C atoms), as a result of a trans addition of acid to the original set of donor atoms in the starting *cis*-platinum(II) complex. The question of whether the position in the octahedron opposite to the apical hydride is occupied by the anion X^- (OTf^-, $BArF^-$, BF_4^-) or by the solvent (CD_3CN) has been solved by observation of the strict similarity of the values of chemical

dx.doi.org/10.1021/ic101879s |*Inorg. Chem.* 2011, 50, 2224–2239

shifts and coupling constants obtained using acids with different anions. A factor of overriding importance in dictating the different patterns in methanol and acetonitrile seems to be the good electron-donor ability of CD_3CN that, as the sixth ligand, concurs to a strong stabilization of the six-coordinate oxidative product. The use of acetonitrile-d_3 to trap five-coordinate transient reaction intermediates onto octahedral species is known.[20]

Interestingly, the values of $^1J_{PtP}$ of the platinum(IV) complexes exhibit an excellent correlation with the electron-donating ability of the Y substituent in the aromatic ring of the benzyl groups, as can be seen from the plot in Figure S5 in the Supporting Information. The best line of the Hammett plot ($^1J_{PtP} = \rho\sigma + C$), in which a rogue point has been omitted, has a slope ρ of 56.3 ± 1.5 Hz, with a correlation coefficient $r = 0.996$. The positive value of ρ suggests that electron withdrawal from substituents results in an increase of the $^1J_{PtP}$ values. An increase in the $^1J_{PtP}$ values has been correlated with a decrease of the Pt−P distance and presumably with an increase of the Pt−P bond strength.[16,21] Similar correlations have been observed for a variety of phosphaneplatinum(II) complexes, but a survey of the literature data indicates that it is difficult to predict the direction and extent of electronic effects on the $^1J_{PtP}$ coupling constants that appear to depend on a multiplicity of variables, such as the nature of the trans-activating group, the nature of groups attached to phosphorus,[22] the chelate ring size,[23] the platinum oxidation state,[24] the Pt−P bond length,[25] and the geometry and charge of the complex.[12a,12c,26]

Oxidative-Addition Reactions. Alkyl- and arylhydridoplatinum(IV) complexes were first proposed as reaction intermediates in early kinetic investigations on the protonolysis of platinum compounds, which were focused almost exclusively on haloalkyl-, diaryl-, and alkylarylplatinum(II) complexes containing soft donor phosphanes.[27] Protonation was thought to take place by (i) a stepwise prior oxidative addition on the central metal followed by reductive elimination [S_E(ox) mechanism] or (ii) a concerted attack at the metal−C bond (S_E2 mechanism), as for electrophilic substitution on main-group organometallics.[28] Because of the microscopic reversibility principle, this issue becomes of overriding importance in the mechanistic elucidation of the activation of alkanes or arenes accomplished using cationic complexes of the type $[PtMe(S)(N{-}N)]^+$,[29] and in some orthometalation reactions using electron-rich organoplatinum(II) reagents.[30] Kinetic studies were unable to solve the problem of the selectivity of the site attack at that time when the intermediates were not detected directly. However, this uncertainty still persists nowadays after the discovery that the protonation of $[PtMe_2(N{-}N)]$ complexes (with N−N typically a bidentate diamine or dimine ligand) with HX leads to the formation of alkylhydridoplatinum(IV) species[31] and other stable methylhydridoplatinum(IV) complexes can be prepared, especially with the use of strongly coordinating *fac*-tridentate ligands.[32] However, the observation of platinum(IV) species could not represent a clear-cut indication of a S_E(ox) mechanism. Tilset et al.[20] have objected that unobserved *kinetic* products could precede a deceptive observation of such hydrides, which could only identify the *thermodynamic* site of protonation rather than the preferred site of protonation. They have suggested a competitive trapping technique to solve the ambiguity.[20]

The choice of the reaction pathway [S_E(ox) or S_E2 mechanism] is still less easy for complexes containing phosphane ligands that are less able to stabilize platinum(IV) species.[33] While the addition of acid to *trans*-$[PtCl(alkyl)(PR_3)_2]$ complexes in a suitable solvent is reported to lead to oxidative-addition products detectable at low temperature,[34,16] for an extensive series of *cis*-$[PtMe_2(PR_3)_2]$, *cis*-$[PtMe(R)(PR_3)_2]$, and *cis*-$[PtMeCl(PR_3)_2]$ complexes, the form of the rate law, the positive large values of the primary isotopic effect, the lack of isotope scrambling with the H atoms belonging to the coordinated alkyl group, and, finally, the failure to observe the formation of platinum(IV) alkylhydride intermediate species in solution were all in favor of a mechanism that entails a rate-determining proton transfer to the Pt−C bond.[16] An identical pattern is observed in this work, when the acidolysis of a *cis*-$[Pt(CH_2Ar)_2(PEt_3)_2]$ (Ar = C_6H_5, **1c**) complex is carried out in methanol and, therefore, metal oxidation and quantitative formation of alkylhydridoplatinum(IV) complexes upon the addition of HOTf or HBArF to *cis*-$[Pt(CH_2Ar)_2(PEt_3)_2]$ (Ar = C_6H_4Y) complexes (1:2, in a CD_3CN solution) came as a surprise to us. Scheme 1 summarizes in a simplified form the two possible alternative reaction pathways and emphasizes the possibility of an easy changeover of the mechanism dictated by rather small differences in the structural properties of the complexes (trans vs cis geometry) or reaction conditions (CD_3OD vs CD_3CN). The basic point is that the energies of **B** and **B′** must have comparable values.

Thus, in methanol, the S_E2 mechanism seems a reasonable hypothesis for *cis*-$[Pt(CH_2Ar)_2(PEt_3)_2]$ (Ar = C_6H_4Y) complexes, while trapping 100% of the product as a platinum(IV) complex in acetonitrile-d_3 is consistent with the initial protonation occurring exclusively at the metal.

Reductive-Elimination Reactions. The principle of microscopic reversibility dictates that the deprotonation step mechanism must occur from the benzylhydridoplatinum(IV). Therefore, reductive elimination of complexes **2a**−**2h**, **C**, evolves along the following steps: (i) dissociation of CD_3CN from the octahedral benzylhydridoplatinum(IV), **C**, to generate a cationic, five-coordinate platinum(IV) intermediate, **B′**, (ii) reductive C−H bond formation producing a platinum(II) alkane σ complex, **D**, and (iii) loss of alkane either through an associative or dissociative substitution pathway to yield the *cis*-$[Pt(CH_2C_6H_4Y)(CD_3CN)(PEt_3)_2]^+$ solvento complex, **E**. This multistep mechanism, involving σ-complex-assisted metathesis, also known as the σ-CAM process,[29a] has gained a general consensus[29b] based on the observation that reductive elimination from **C**, except rare cases,[35] requires ligand dissociation[27,36] with the formation of a square-pyramidal five-coordinate structure **B′**.[37]

Reductive elimination results in a σ complex that so far is supported by kinetic data and isotopic labeling experiments[38] and only by a little other indirect experimental evidence, such as time-resolved IR spectroscopy on the nanosecond scale[39] or the detection of metastable minima in several theoretical investigations of C−H bond activation.[40] The observation of a mass-law retardation of the rates of reductive elimination with an increase in the amount of CD_3CN in CD_2Cl_2/CD_3CN mixtures is consistent with dissociation as a preliminary step for the reaction. The lack of isotope scrambling with the methylene H atoms belonging to a coordinated benzyl group, observed during the deuterolysis measurements, leads to the conclusion that the nucleophilic attack by CD_3CN at the alkane σ complex **D** must be very fast and, in any case, much faster than the reverse process, preventing a scrambling equilibrium. There is no evidence here, as in many other cases,[41] of any involvement as intermediates of coordinatively unsaturated three-coordinate, T-shaped platinum(II) species **D′**. The latter, however, were shown to play a fundamental role in initiating the concerted oxidative addition of the alkane C−H bonds in some electron-rich platinum(II) organometallic complexes.[42,30]

Scheme 1. Alternative Reaction Pathways for Acidolysis of an Alkylplatinum(II) Complex

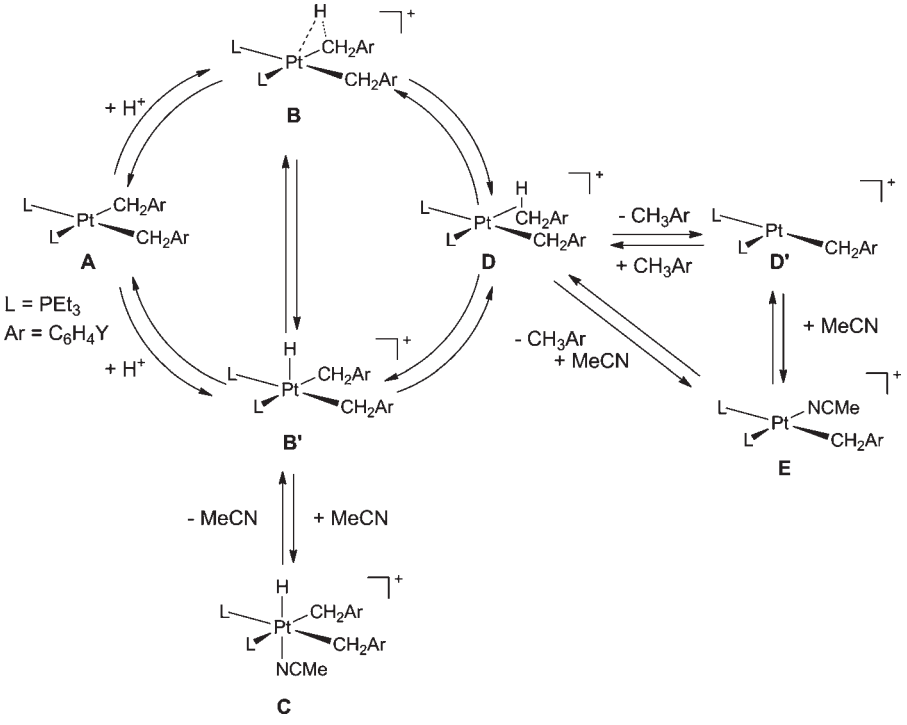

We found that the rate constant for 4-F-toluene elimination from **2d** is 7.78×10^{-4} s^{-1} at 233.4 K in acetonitrile-d_3. The temperature dependence of this reaction was studied over the range 230−255 K, and the pseudo-first-order rate constants k_{obsd} were fitted to the Eyring equation to yield the values of the activation parameters $\Delta H^{\ddagger} = 63.8 \pm 3.5$ kJ mol^{-1} and $\Delta S^{\ddagger} = -29.0 \pm 14.6$ J K^{-1} mol^{-1}. These activation parameters can be compared with those of reductive elimination of toluene from [(tmeda)Pt(CH_2Ph)(H)Cl_2] (tmeda = *N*,*N*,*N*′,*N*′-tetramethylethylenediamine) in CD_2Cl_2, $\Delta H^{\ddagger} = 58.6 \pm 10$ kJ mol^{-1} and $\Delta S^{\ddagger} = -77.4 \pm 30$ J K^{-1} mol^{-1} reported by Stahl et al.[31c] The observed large negative activation entropies contrast with the idea that elimination reactions should be accompanied by very positive activation entropies and confirm a mechanism other than a simple direct reductive elimination from six-coordinate platinum(IV). Electrostriction effects and ordering of solvent molecules accompanying dissociation of a ligand from the octahedral six-coordinate platinum(IV) can well account for a negative value of the activation entropy.[43]

Isomerization: Kinetic Studies. In acetonitrile-d_3, the spontaneous cis-to-trans geometrical conversion of **3a**−**3h**, resulting from the reductive elimination of the corresponding benzylhydridoplatinum(IV) compounds, can be monitored quite easily in the 260−280 K temperature range by NMR measurements (see Figure 4). For all of the compounds, the conversion is complete, stable trans isomers are the only species at the end of the reaction, and the kinetics can be examined by using the time dependence of the fraction of reaction (F) of the label. However, the systematic kinetics were obtained by stopped-flow spectrophotometric measurements in a temperature range (285−320 K) where the oxidative-addition/reductive-elimination process is very fast and acidolysis of the precursors dibenzyl complexes **1a**−**1h** gives directly the cationic *cis*-[Pt(CH_2Ar)(CH_3CN)(PEt_3)$_2$]$^+$ solvento complexes. The

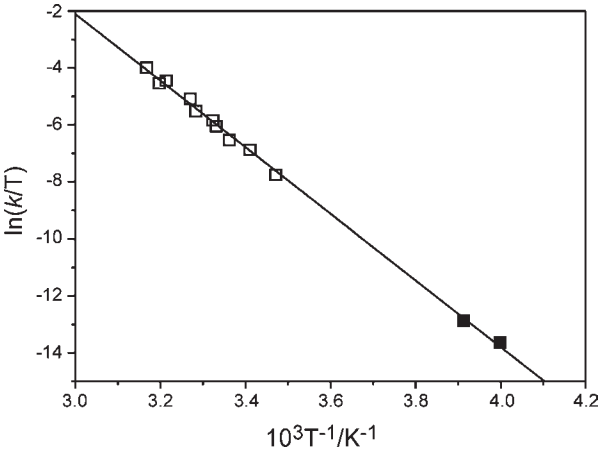

Figure 5. Eyring plot for the isomerization reaction of **3d** constructed by the use of rate data obtained with different techniques (empty squares from stopped-flow spectrophotometric experiments; full squares from ^{1}H NMR experiments).

variable-temperature rate constants for compound **3d** obtained with the two techniques were fitted to the Eyring equation (Figure 5), leading to $\Delta H^{\ddagger} = 97 \pm 2$ kJ mol^{-1}, $\Delta S^{\ddagger} = 76 \pm 4$ J K^{-1} mol^{-1}, and $\Delta G^{\ddagger}_{298} = 74.4 \pm 0.8$ kJ mol^{-1}.

The whole set of kinetic data and activation parameters for **3a**−**3h** compounds is collected in Table 5. Typically, the geometrical conversion of these solvento complexes appears to be characterized by large positive values of the entropy of activation, confirming previous findings on similar systems. Therefore, the well-established dissociative mechanism illustrated in Scheme 2 applies, which involves dissociative loss of

dx.doi.org/10.1021/ic101879s |*Inorg. Chem.* 2011, 50, 2224–2239

Table 5. Effect of Variation of the Nature of Ar and of the Solvent on the Computed Relative Energies (kJ mol^{-1}) of the Optimized Structures of the Reactant, the T-Shaped Reaction Intermediates, the TSs for Their Fluxionality, and the Product during Isomerization of *cis*-$[Pt(CH_2Ar)(S)(PEt_3)_2]^+$ (S = Solvent) Complexes[a]

no.	Ar	S	T-shaped cis	TS	T-shaped trans	trans product
3c	C_6H_5	CH_3CN	36.2	66.7	50.6	−18.6
3f	4-ClC_6H_4	CH_3CN	39.7	70.8	54.7	−16.9
3a	4-$CH_3C_6H_4$	CH_3CN	29.1	60.5	45.5	−19.7
3c	C_6H_5	MeOH	10.9	41.3	25.2	3.30
3f	4-ClC_6H_4	MeOH	10.4	41.6	25.4	−3.47

[a] All relative energy values are calculated with respect to the original cationic solvento complex.

Scheme 2. Mechanism for the Isomerization of Cationic Solventoplatinum(II) Complexes

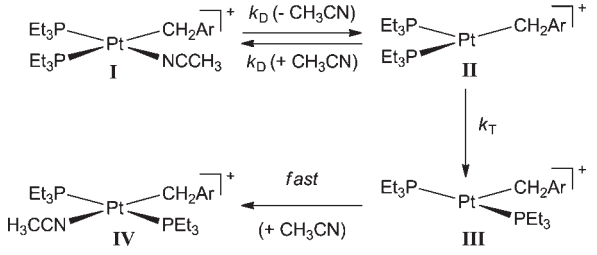

the solvent molecule and interconversion of two geometrically distinct three-coordinate, T-shaped, 14-electron intermediates.

A rate law of the form

$$k_i = \frac{k_D}{1 + (k_{-D}/k_T)[S]} \qquad (5)$$

can be derived, in which the term $(k_{-D}/k_T)[S]$ measures the retardation due to capture of the first intermediate by the bulk solvent.[44]

The mechanism and the rate law account for the crucial role played by the nature of the solvent in such reactions whose rate can be finely tuned through appropriate control of the coordinating properties of the leaving group.[45] Other main factors that usually combine in affecting the rate of conversion are (i) the stereoelectronic properties of the phosphane ligands[12a,12c] and (ii) interaction of the β-H atoms of the alkyl chain with the coordinatively unsaturated intermediate. The sharp acceleration of the reaction rate produced by such agostic interactions has been defined as the "β-hydrogen kinetic effect".[11] We observe that the rate of isomerization of the benzyl *cis*-solvento $[Pt(CH_2Ar)(CH_3CN)(PEt_3)_2]^+$ complexes (Ar = C_6H_5; $k_i = 0.820\ s^{-1}$, $\Delta H^{\ddagger} = 83.8 \pm 1.3$ kJ mol^{-1}, $\Delta S^{\ddagger} = 34.6 \pm 4$ J K^{-1} mol^{-1}, and $\Delta G^{\ddagger}_{298} = 73.5 \pm 0.1$ kJ mol^{-1}) is higher than that of the ethyl $[Pt(C_2H_5)(CH_3CN)(PEt_3)_2]^+$ complex ($k_i = 4.9 \times 10^{-3}\ s^{-1}$, $\Delta H^{\ddagger} = 100.5$ kJ mol^{-1}, $\Delta S^{\ddagger} = 48.2$ J K^{-1} mol^{-1}, and $\Delta G^{\ddagger} = 86.1$ kJ mol^{-1}) and is several orders of magnitude higher than that of the methyl $[Pt(CH_3)(CH_3CN)(PEt_3)_2]^+$ complex ($k_i = 2.42 \times 10^{-6}\ s^{-1}$, $\Delta H^{\ddagger} = 147.7$ kJ mol^{-1}, $\Delta S^{\ddagger} = 139$ J K^{-1} mol^{-1}, and $\Delta G^{\ddagger} = 106.3$ kJ mol^{-1}).[11] Thus, the rate increases markedly along the series R, $CH_3 \ll C_2H_5 < CH_2C_6H_5$, in the ratio 1:2000:340 000, giving a clear-cut indication of a stabilization energy of the reaction TS/intermediate higher than that of the agostic interaction caused by interactions of the unsaturated metal with the benzyl moiety. On the basis of the values of the free activation energies, the stabilization energy of an agostic TS relative to that of a nonagostic TS (as for the methyl compound) is about 20 kJ mol^{-1}, while the extra TS energy stabilization induced by interactions with a benzyl group is in the range of 10−15 kJ mol^{-1}.

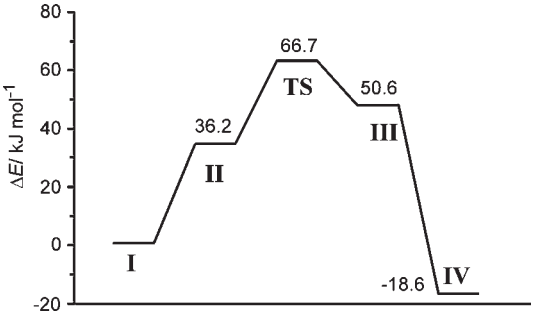

Figure 6. Calculated DFT energy profile for isomerization of the cationic solvento complex $[Pt(CH_2C_6H_5)(CH_3CN)(PMe_3)_2]^+$.

Isomerization: DFT Studies. The energy profile for the geometrical isomerization of *cis*-$[Pt(CH_2C_6H_5)(CH_3CN)(PMe_3)_2]^+$ is given in Figure 6 as a typical example of the shape obtained from DFT calculations for a variety of systems. Relative energies are calculated with respect to the energy of the *cis*-$[Pt(CH_2C_6H_5)(CH_3CN)(PMe_3)_2]^+$ complex indicated as **I**. In Figure 7 are shown the fully optimized geometrical structures of minima and TS along with the most relevant calculated geometrical parameters. The process is assumed to evolve along the same key steps as those indicated in Scheme 2, that is, (i) ligand dissociation, (ii) conversion of a three-coordinate, T-shaped intermediate from a "cis-like" to a "trans-like" geometry, and (iii) final uptake of the ligand by the latter.

The overall set of DFT data for the studied systems is given in Table 5, which reports the relative energies of intermediates, of the TS corresponding to the cis-to-trans rearrangement and of the product.

Upon comparison of these data with those of the agostic analogues reported in ref 11, we see that the first reaction step, namely, extrusion of the molecule of solvent from *cis*-$[Pt(R)(CH_3CN)(PEt_3)_2]^+$ complexes, is energetically easier when R = $CH_2C_6H_5$ than when R = C_2H_5, combining a greater lability of the CH_3CN solvent with respect to methanol with a greater stability of the three-coordinate *cis*-$[Pt(CH_2C_6H_5)(PEt_3)_2]^+$ complex.

Conversion from a cis-like to a trans-like T-shaped configuration occurs via a TS that possesses a Y-shaped configuration and usually requires a very low energy.[46] The energy barrier associated with the rearrangement of *cis*-$[Pt(R)(PEt_3)_2]^+$, when the R group does not contain β-hydrogens (R = Me), is very small (average = 9.1 ± 0.4 kJ mol^{-1}).[11] It is doubled (average =18.9 ± 2 kJ mol^{-1}) when the R group does contain β-hydrogens (R = Et, Bu) and, when R = benzyl, becomes still greater (average 30.9 ± 0.4 kJ mol^{-1}). Thus, conversion of an agostic "cis-like" three-coordinate form to its trans form requires a supplementary consumption of energy. This additional energy request is increased further when a $-CH_2Ph-$metal bond is involved, and it becomes comparable with the dissociation energy of the solvent from the coordination sphere of the metal. Another peculiarity of the potential energy surface (PES) shown in Figure 6, still depending upon the strong stability conferred by the benzyl−metal bond to the "cis-like" intermediate, is given by the fact that intermediate **II** is about 15 kJ mol^{-1} more stable than intermediate **III**, while methyl and ethyl complexes show a reverse trend.

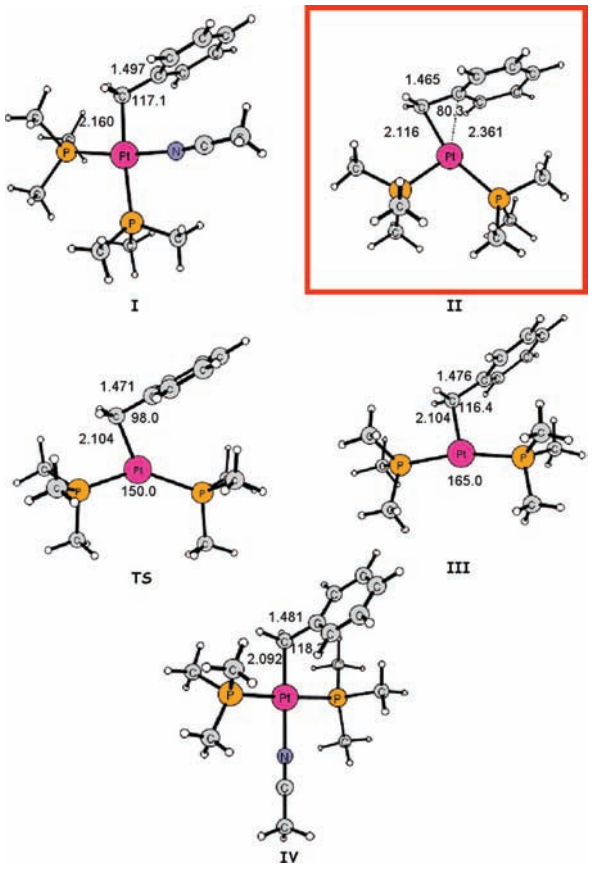

Figure 7. Fully optimized geometrical structures of stationary points intercepted along the energy profile for isomerization of the cationic solvento complex $[Pt(CH_2C_6H_5)(CH_3CN)(PMe_3)_2]^+$. Bond lengths are in angstroms and angles in degrees.

In Figure 7 are shown the optimized structures of the stationary points of Figure 6.

Both **I** and **IV**, the starting cis-solvento and the final trans-solvento $[Pt(R)(CH_3CN)(PMe_3)_2]^+$ cationic complexes, show the expected geometrical features with bond separations and angles comparable to those of similar structurally characterized compounds, including the dibenzyl precursors shown in Figures 1 and 2. The benzyl ligand in each of the complexes is normal, exhibiting a $M-CH_2$ single bond length of 2.160 Å in **I** and 2.092 Å in **IV** and a pseudotetrahedral environment around its methylene C atom. Jahn−Teller instability favors a T-shaped configuration for both "cis-like" **I** and "trans-like" three-coordinate $[Pt(CH_2C_6H_5)(PMe_3)_2]^+$ (**IV**) species, which mutually convert passing through a Y-shaped transition state **TS**.

Stabilization of Transient Three-Coordinate Species. It is established that the labile existence of unsaturated 14-electron intermediates is favored by several factors such as strong σ-donating ligands, overcrowding of coordination sphere, and agostic interactions. The most chemically interesting feature of the computed structures displayed in Figure 7 is that in the present case formation of an η^2 bond that involves the benzyl ligand and the unsaturated metal is responsible of stabilization of the "cis-like" T-shaped, three-coordinate intermediate **II**. The "dihapto" bonding mode is characterized by the following distinctive parameters: (i) the metal−methylene bond length (2.116 Å) is in the range expected for a normal $Pt^{II}-C$ single bond, (ii) the $M-C_{ipso}$ distance (2.361 Å) is not very far away from this value, (iii) the angle at the methylene C atom ($Pt-CH_2-C_{ipso}$) is well below the value expected for a tetrahedral sp^3 C environment, being 80.3°, and (iv) its two $M-C_{ortho}$ distances (2.73 and 3.21 Å) are much longer than those commonly observed for platinum(II), palladium(II), or nickel(II) complexes containing η^3-CH_2Ph groups consistent with an allyl type of bonding where the Pt−C distances to the outer allylic C atoms range from 2.110 to 2.449 Å.[47] In Table 6, we report for comparison some significant $M-C_{ipso}$, $M-C_{ortho}$, and $M-C_1$ distances (Å) for selected platinum(II), palladium(II), or nickel(II) η^3-benzyl complexes. In some of these complexes, the benzyl group is bonded to the metal in an unsymmetrical fashion, with the metal−C bond length increasing in the order $M-CH_2 < M-C_{ipso} < M-C_{ortho}$; however, the $M-C_{ortho}$ distance does not exceed 2.446 Å. Other interesting platinum(II) compounds with an allyl type of bonding are the dinuclear $[\{Pt(Et_2PC_2H_4PEt_2)\}_2(\mu$-biphenyl)$][BArF]_2$ complex,[48] and some η^3-bonded platinum benzyl cations $[Pt(N-N)(CH_2C_6H_5]^+$, where N−N represents a bidentate diimine ligand, that have been identified by NMR in solution.[49] We performed a DFT optimization of one simplified form of such cationic complexes, shown in Figure 8, which confirms that the benzyl anion is in an η^3-bonded mode, with M−C distances increasing slightly along the series $M-CH_2$, 2.10 Å < $M-C_{ipso}$, 2.26 Å < $M-C_{ortho}$, 2.35 Å.

The energy stabilization associated with the presence of a metal−η^2-benzyl linkage in the transient cis-like T-shaped

Table 6. Comparison of the Intramolecular Dimensions in Some Structurally Characterized Metal η^3-Benzyl Complexes

complex	M−CH_2[a]	M−C_{ipso}[b]	M−C_{ortho}[c]	ref
$[Pt(dbpp)(\eta^3$-*anti*-1-$MeCHC_6H_4$-*p*-Br)]	2.163	2.242	2.446	47a
$[Pt(BAB)(\eta^3$-1-$MeCHC_6H_5)]$	2.118	2.145	2.110	47b
$[Pt(acac)(\eta^3$-$CPh_3)]$	2.088	2.120	2.148	47c
$[Pd(phen)(anti$-η^3-$CH(CH_2CH_3)C_6H_5)]BArF$	2.117	2.135	2.251	47d
$[Pd(dipy)(\eta^3$-*syn*-α-$(CH_3)CHC_6H_5)]$	2.08	2.13	2.28	47e
$[Ni(\eta^3$-$CH_2C_6H_4$-*o*-Me)$ClPMe_3]$	1.930	2.050	2.318	47f
$[Ni(\eta^3$-$CH_2C_6H_4$-*p*-$CF_3)$(dippm)]	1.981	2.044	2.185	47g
$Ni(\eta^3$-$CH_2C_6H_5)[Ph_2PC_6H_4C$-$(O-B(C_6F_5)_3)O$-κ^2-*P*,*O*]	1.944	2.064	2.198	47i

[a] Metal to methylene carbon bond length. [b] Metal to *ipso*-carbon bond length. [c] Shortest metal to *o*-carbon bond distance.

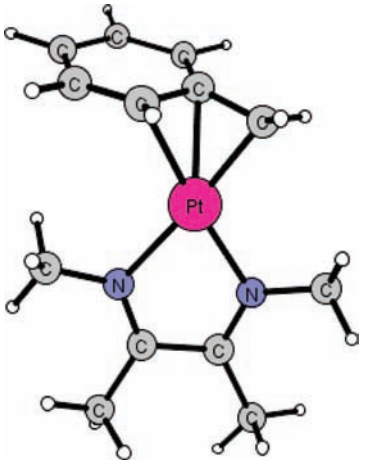

Figure 8. Optimized DFT structure of $[(MeN{=}C(Me)C(Me){=}NMe)Pt(\eta^3$-$CH_2C_6H_5)]^+$.

intermediate has been estimated starting from the fully optimized structure of the *cis*-$[Pt(CH_2C_6H_5)(MeOH)(PEt_3)_2]^+$ solvent complex and performing a relaxed scan calculation of the Pt−O bond length, while MeOH leaves the coordination sphere of the metal.[50] The stabilization energy amounts to 31.8 kJ mol^{-1} and compares well with the value of the agostic stabilization energy (24.5 kJ mol^{-1}) calculated using a similar method.[11] Thus, there is a substantial agreement between the kinetic and computational data, indicating in ≈10−15 kJ mol^{-1} the energy difference between the incipient β-agostic and the incipient *ipso*-carbon interactions shown in Figure 9.

Table 7 gives a summary of the kinetic and calculated activation data. The presence of a preequilibrium and of a retardation term $(k_{-D}/k_T)[S]$ in the rate law complicates the kinetics, and the resulting k_{obs}, from which the kinetic activation data are derived, is a composite rate constant that contains equilibrium constants and rate constants for elementary steps. In constrast, theoretical calculations refer only to elementary steps. Thus, we cannot expect a strict analogy between kinetic and computational data, in their absolute values but only good correlations and similar trends. As an example, an excellent straight line correlates the calculated (*cis*-$[Pt(R)(CH_3CN)(PMe_3)_2]^+$) and experimental values of free energy of activation for isomerization of *cis*-$[Pt(R)(CH_3CN)(PEt_3)_2]^+$ (R = Me, Et, Bz). The plot is reported as Figure S6 in the Supporting Information.

Leaving-Group and Substituent Effects. The theoretical data in Table 6 confirm the experimental findings. The energy involved in the formation of the "cis-like" T-shaped, 14-electron, three-coordinate intermediate (see data) depends on the nature of the leaving group, with the sequence of lability being $CH_3CN \ll$ MeOH. This confirms the key role that dissociation of the solvent from platinum(II) plays in the energetics of the overall process and in the different observed reaction pathways.

Both kinetic and DFT data indicate that isomerization is strongly affected by the amount of electron density at the metal

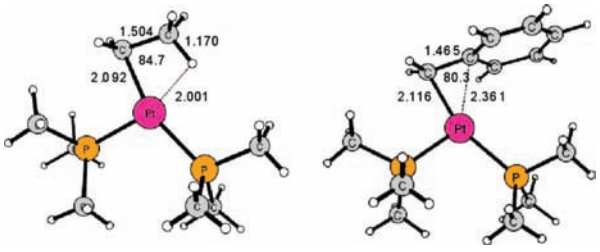

Figure 9. Optimized structures of the agostic $[Pt(PMe_3)_2(ethyl)]^+$ and of $[Pt(PMe_3)_2(\eta^2\text{-benzyl})]^+$ intermediates.

Table 7. Summary of Kinetic and Theoretical Data for the Geometrical Isomerization of *cis*-$[PtL_2(R)(CH_3CN)]^+$ Complexes

R	k_i[a,b]	$\Delta H^{\ddagger}$[a,c]	$\Delta S^{\ddagger}$[a,d]	$\Delta G^{\ddagger}$[a,e]	stabilization energy[f,g]	$\Delta H^{\ddagger}$[c,f,g]
Me	2.42×10^{-6}	148	139	106		116
Et	4.90×10^{-3}	100	48	86	25	91
Bz	0.820	84	35	73	35	67

[a] L = PEt_3. [b] First-order rate constant in s^{-1} at 298.2 K. [c] Enthalpies of activation in kJ mol^{-1}. [d] Entropies of activation in J K^{-1} mol^{-1}. [e] Free energy of activation in kJ mol^{-1} at 298.2 K. [f] L = PMe_3. [g] From theoretical calculations.

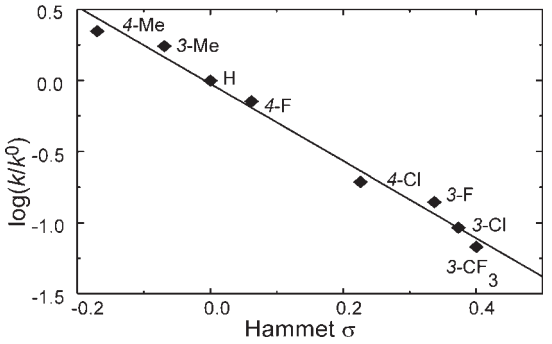

Figure 10. Dependence of the rates of isomerization (k_i at 298.2 K) of *cis*-$[Pt(PEt_3)_2(CH_2C_6H_4Y)(CD_3CN)]^+$ complexes upon the electron-donor properties of Y substituents on the aromatic ring.

Table 8. Experimental Data for the X-ray Diffraction Study of Compounds 1a and 1f

	1a	1f
formula	$C_{28}H_{48}P_2Pt$	$C_{26}H_{42}Cl_2P_2Pt$
mol wt	641.69	682.53
data collecn *T*, K	295(2)	295(2)
diffractometer	Bruker SMART CCD	
cryst syst	monoclinic	monoclinic
space group	*C*2/*c* (No. 15)	*Cc* (No. 9)
a, Å	16.596(2)	12.592(1)
b, Å	10.149(1)	31.223(3)
c, Å	17.844(2)	8.4416(9)
β, deg	100.179(2)	120.802(2)
V, Å^3	2958(2)	2850.6(9)
Z	4	4
ρ_{calcd}, g cm^{-3}	1.441	1.590
μ, cm^{-1}	4.864	5.234
radiation	Mo Kα (graphite monochromator, λ = 0.710 73 Å)	
θ range, deg	2.32 < θ < 26.02	1.99 < θ < 26.02
no. of data collected	12964	12487
no. of independent data	2907	5573
no. of obsd reflns (n_o) [$\lvert F_o\rvert^2 > 2.0\sigma(\lvert F\rvert^2)$]	2742	5000
no. of refined param (n_v)	141	280
R_{int}	0.0310	0.0286
R (obsd reflns)	0.0174	0.0270
wR2 (obs reflns)	0.0434	0.0601
GOF	1.113	1.047
absolute structure param (Flack)		−0.009(7)

[a] $R_{int} = \sum|F_o^2 - \langle F_o^2\rangle|/\sum\Sigma F_o^2$. [b] $R = \sum(|F_o - (1/k)F_c|)/\sum|F_o|$. [c] wR2 = $\{\sum[w(F_o^2 - (1/k)F_c^2)^2]/\sum w|F_o^2|^2]\}^{1/2}$. [d] GOF = $[\sum_w(F_o^2 - (1/k)F_c^2)^2/(n_o - n_v)]^{1/2}$.

atom, brought about by substituents on the aromatic ring. Electron-donating substituents on the aromatic ring enhance the rate of isomerization of the complexes *cis*-$[Pt(PEt_3)_2(CH_2C_6H_4Y)(CD_3CN)]^+$, while electron-attracting groups have the reverse effect. The kinetic data for the isomerization fit a rather good Hammett plot fitting the equation $\log(k/k_H) = \rho\sigma + C$. The best line has a slope ρ of −2.71, with a correlation coefficient r = −0.993 (Figure 10).

The constant ρ measures the sensitivity of the isomerization to electronic effects transmitted by meta and para substituents on the aryl ring, and it is of the expected sign and magnitude because electron-donating (negative σ) substituents facilitate the departure of CD_3CN with its previously bonding electron pair by stabilizing a TS similar to that of the electron-deficient platinum cation.

dx.doi.org/10.1021/ic101879s |*Inorg. Chem.* 2011, 50, 2224–2239

An analogous result stems from the DFT study, which indicates that the energy of the TS for isomerization of *cis*-[Pt(PEt_3)(CH_2-C_6H_4Y)(CD_3CN)]$^+$ decreases in the order of the electron-donor capacity of the substituent Y (Y = 4-CH_3 > H > 4-Cl), reflecting the efficiency of the substituents in stabilizing the three-coordinate platinum(II) cationic TS (Figure S8 in the Supporting Information).

CONCLUSIONS

In this study, the different kinetic behavior of meta- and para-substituted dibenzylplatinum(II) complexes *cis*-[Pt(CH_2Ar)$_2$-(PEt_3)$_2$] upon protonolysis and deuterolysis by H(D)X acids in methanol or in acetonitrile-d_3 as solvents is described. Low-temperature NMR spectra recorded in CD_3OD show that the reactions lead directly to the formation of the corresponding solvento species *trans*-[Pt(CH_2Ar)(PEt_3)$_2$(CD_3OD)]X and toluene derivatives. Instead, in acetonitrile-d_3, a suitable temperature increase allows one to kinetically distinguish three subsequent stages, such as the instantaneous formation of new benzylhydridoplatinum(IV) complexes *cis*-[Pt(CH_2Ar)$_2$(H)-(CD_3CN)(PEt_3)$_2$]X (at 230 K), followed by reductive elimination to yield *cis*-[Pt(CH_2Ar)(CD_3CN)(PEt_3)$_2$]X and toluene derivatives (in the range 230−255 K), and finally spontaneous isomerization of the cis-cationic solvento species to the corresponding trans isomers (in the range 260−280 K).

Furthermore, this work shows by a kinetic and theoretical approach that the energy of T-shaped, three-coordinate species, formed upon ligand dissociation from a square-planar platinum(II) complex, can be modulated by control of electron donation to the metal through secondary interactions. Because of its coordinative and electronic unsaturation, the metal shows a great tendency to interact with that part of a coordinated ligand that can satisfy this requirement, such as the C−H bond of a dangling coordinated alkyl or the *ipso*-C of a benzyl group. The onset of such secondary interactions is indicated by a marked increase of the rate of reaction and can be rationalized by geometry optimization and DFT energy calculation of the species intercepted at the stationary points of the PESs. We observe that there is an energetic hierarchy in such interactions, with the bond with an *ipso*-C being stronger than that with a C−H bond, even though for both of them it should be more appropriate to speak in terms of "incipient" interactions. As a matter of fact, the β-hydrogen kinetic effect is characterized by an intrinsic energetic weakness of the agostic bond in the ethyl intermediate, while in the "ipso-carbon kinetic effect", the presence of an η^2-benzyl bond in the benzyl intermediate reflects the difficulty of developing a stronger η^3-allyl-type bond. In light of the extreme electrophilicity of the metal in a coordinatively unsaturated metal d^8 three-coordinate 14-electron species, and of its tendency to stabilize intramolecular interactions, its fate in solution is quite unpredictable. As a matter of fact, such labile intermediate species can undergo a number of different processes as follows: (i) easy attack or reentry in the coordination sphere by even very weak nucleophiles such as a solvent molecule; (ii) a topological process that changes the T-shaped geometry; (iii) intraligand processes such as C−H bond activation, β-hydrogen elimination, η^1 to η^3 fluxional changes, etc. Because of the great interest in the possibility of considering alternative low-energy pathways involving these unsaturated electronically and coordinavely unsaturated ML_3 species, the fine-tuning of the electronic request by the metal, through a rationale choice of the coordinated ligands, can open the way to control of the rates and the stereospecificity of many fundamental processes.

EXPERIMENTAL SECTION

General Procedures and Chemicals. All manipulations were performed in a drybox under a dry and oxygen-free dinitrogen atmosphere in glassware that had been oven-dried or by using standard Schlenk techniques. Unless otherwise noted, all reagents were commercially obtained and, where appropriate, purified prior to use. Tetrahydrofuran, diethyl ether, and toluene (analytical reagent grade, Lab-Scan Ltd.) were distilled under nitrogen from sodium benzophenone ketyl. Dichloromethane was distilled from barium oxide.[51] Phosphane ligands (from Strem), acetonitrile spectrophotometric grade for kinetic studies, CD_3CN, CD_3OD, CH_3OD, and DOTf for NMR measurements were used as received from Aldrich Chemical Co. HB{[3,5-C_6H_3-(CF_3)$_2$)$_4$]} (HBArF) was prepared by the Brookhart method.[52] Platinum dibenzyl complexes were stored in a drybox under a dinitrogen atmosphere.

Instrumentation and Measurements. Microanalyses were performed by the Microanalytical Laboratory, University of Dublin, Dublin, Ireland. ^{1}H and ^{31}P NMR spectra were recorded on a Bruker AMX-300 spectrometer. The ^{1}H resonance of the solvent was used as an internal standard, but chemical shifts are reported with respect to Me_4Si. $^{31}P\{^1H\}$ NMR shifts are referenced to external 85% H_3PO_4. The data are reported as follows: chemical shift in ppm (δ) units, multiplicity, coupling constants (Hz), and integration. The temperature within the probe was checked using the methanol method.[53] Electronic spectra of the solutions were taken with a rapid-scanning Hewlett-Packard model 8452A spectrophotometer or a Jasco V-560 UV−vis spectrophotometer. Fast reactions required the use of an Applied Photophysics Bio Sequential SX-17 MX stopped-flow ASVD spectrofluorometer. Rate constants were evaluated by the Applied Photophysics software package[54] and are reported as average values from five to seven independent runs.

Dibenzyl Complexes. The complex *cis*-[Pt(CH_2Ar)$_2$(PEt_3)$_2$] (Ar = C_6H_5, **1c**) was prepared according to the literature method.[12] The complexes (Ar = 4-Me-C_6H_4, **1a**; 3-Me-C_6H_4, **1b**; 4-F-C_6H_4, **1d**; 3-F-C_6H_4, **1e**; 4-Cl-C_6H_4, **1f**; 3-Cl-C_6H_4, **1g**; 3-CF_3-C_6H_4, **1h**) are new and were synthesized according to a general procedure as follows. An ethereal suspension of *cis*-[$PtCl_2$(PEt_3)$_2$] (400 mg, 0.8 mmol) at 0 °C and under an inert atmosphere was treated with a stoichiometric amount of Grignard reagent, prepared from magnesium and the appropriate benzyl halide. The mixture was stirred at 20 °C for 2 h and then hydrolyzed with ice. The crude product isolated from the dried (Na_2SO_4) organic layer by evaporation of the residual solvent under reduced pressure was recrystallized from a dichloromethane/methanol mixture. The identity and purity of the these compounds were established by elemental analysis and by ^{1}H and $^{31}P\{^1H\}$ NMR spectra. Elemental analyses were consistent with the theoretical formulas.

***cis*-[Pt($CH_2C_6H_4$-4-Me)$_2$(PEt_3)$_2$] (1a).** Yield: 88.0%. Anal. Calcd for $C_{28}H_{48}P_2Pt$: C, 52.41; H, 7.54. Found: C, 51.21; H, 7.36. ^{1}H NMR (CH_3CN-d_3, T = 298 K): δ 7.06 (d, 4H, $^3J_{HH}$ = 7.5 Hz, $H_{2,6}$), 6.83 (d, 4H, $^3J_{HH}$ = 7.5 Hz, $H_{3,5}$), 2.39 (m, 4H, $^2J_{PtH}$ = 83.4 Hz, $^3J_{PH}$ = 16.9 Hz, Pt−CH_2), 2.12 (s, 6H, Ph−CH_3), 1.74 (m, 12H, $^3J_{HH}$ = 7.5 Hz, P−CH_2), 0.96 (m, 18H, $^3J_{HH}$ = 7.5 Hz, P−CH_3). $^{31}P\{^1H\}$ NMR (CH_3CN-d_3, T = 298 K): δ 12.5 ($^1J_{PtP}$ = 1943 Hz).

Alkylhydridoplatinum(IV) Species 2a−2h. A solution of an appropriate amount of **1a**−**1h** (5−6 mg, ca. 10 μmol) in CH_3CN-d_3 (ca. 400 μL) was cooled to −78 °C in an NMR tube and accurately layered with a solution of 2 equiv of acid (HOTf, HBArF, or $HBF_4\cdot Et_2O$) in CH_3CN-d_3. While keeping the tube as cool as possible, it was capped and shaken to mix the contents immediately before transfer to a precooled NMR probe. Relevant ^{1}H and ^{31}P NMR data for *cis*-[Pt(CH_3CN)(H)-($CH_2C_6H_4Y$)$_2$(PEt_3)$_2$]$^+$ species are listed in Table 1.

dx.doi.org/10.1021/ic101879s |*Inorg. Chem.* 2011, 50, 2224–2239

***cis*-[Pt(CH$_2$C$_6$H$_4$-4-Me)$_2$(H)(CD$_3$CN)(PEt$_3$)$_2$](BArF) (2a).** ^{1}H NMR (CH$_3$CN-d_3, T = 238.5 K): δ 7.14−6.65 (m, 8H, $H_{2,6}$ + $H_{3,5}$), 2.35 (m, 4H, $^2J_{PtH}$ = 65.5 Hz, $^3J_{PH}$ = 14.9 Hz, Pt−CH_2), 1.79 (m, 12H, $^3J_{HH}$ = 8.9 Hz, P−CH_2), 2.08 (s, 6H, Ph−CH_3), 0.96 (m, 18H, $^3J_{HH}$ = 8.9 Hz, P−CH_3), −21.4 (m, 1H, $^1J_{PtH}$ = 1271 Hz, $^2J_{PH}$ = 26.8 Hz, Pt−H). ^{31}P{^{1}H} NMR (CH$_3$CN-d_3, T = 238.5 K): δ −3.5 ($^1J_{PtP}$ = 1188 Hz).

Monoalkyl Solvento Complexes *cis*-[Pt(CH$_2$C$_6$H$_4$Y)(CD$_3$CN)(PEt$_3$)$_2$]$^+$ (3a−3h). Upon a gentle increase of the temperature in the range 230−255 K, the alkylhydridoplatinum(IV) species **2a**−**2h** of the previous experiment undergo easy reductive elimination. The ^{1}H and ^{31}P NMR spectra of the ensuing toluene derivatives and *cis*-monobenzylsolvento species were recorded and resonances assigned.

***cis*-[Pt(CH$_2$C$_6$H$_4$-4-Me)(CD$_3$CN)(PEt$_3$)$_2$]$^+$ (3a).** ^{1}H NMR (CH$_3$-CN-d_3, T = 238.5 K): δ 6.97 (d, 2H, $^3J_{HH}$ = 8.8 Hz, $H_{2,6}$), 6.87 (d, 2H, $^3J_{HH}$ = 8.8 Hz, $H_{3,5}$), 2.29 (m, 2H, $^2J_{PtH}$ = 60.2 Hz, $^3J_{PH}$ = 8.8 Hz, Pt−CH_2), 2.04 (s, 3H, Ph−CH_3), 1.74 (m, 6H, $^3J_{HH}$ = 7.5 Hz, P$_A$−CH_2), 1.63 (m, 6H, $^3J_{HH}$ = 7.5 Hz, P$_B$−CH_2), 0.90 (m, 9H, $^3J_{HH}$ = 7.5 Hz, P$_A$−CH_3), 0.80 (m, 9H, $^3J_{HH}$ = 7.5 Hz, P$_B$−CH_3). ^{31}P{^{1}H} NMR (CH$_3$CN-d_3, T = 238.5 K): δ 16.9 (d, $^1J_{PtP}$ = 1790 Hz, $^2J_{P_AP_B}$ = 17.80 Hz, P$_A$ trans to the benzyl group), 12.2 (d, $^1J_{PtP}$ = 4142 Hz, $^2J_{P_AP_B}$ = 17.80 Hz, P$_B$ trans to CD$_3$CN).

Monoalkyl Solvento Complexes *trans*-[Pt(CH$_2$C$_6$H$_4$Y)(CD$_3$-CN)(PEt$_3$)$_2$]$^+$ (4a−4h). Spontaneous conversion of the cis-solvento isomers **3a**−**3h** into their corresponding trans derivatives was obtained easily by setting aside at room temperature the solution resulting from the electrophilic attack on the corresponding dibenzyl precursors. The process goes to completion in a few seconds.

***trans*-[Pt(CH$_2$C$_6$H$_4$-4-Me)(CD$_3$CN)(PEt$_3$)$_2$]$^+$ (4a).** ^{1}H NMR (CH$_3$CN-d_3, T = 298 K): δ 7.22 (d, 2H, $^3J_{HH}$ = 7.5 Hz, $H_{2,6}$), 6.98 (d, 2H, $^3J_{HH}$ = 7.5 Hz, $H_{3,5}$), 2.60 (m, 2H, $^2J_{PtH}$ = 98.1 Hz, $^3J_{PH}$ = 16.9 Hz, Pt−CH_2), 2.27 (s, 3H, Ph−CH_3), 1.73 (m, 12H, $^3J_{HH}$ = 7.5 Hz, P−CH_2), 1.06 (m, 18H, $^3J_{HH}$ = 7.5 Hz, P−CH_3). ^{31}P{^{1}H} NMR (CH$_3$CN-d_3, T = 298 K): δ 20.8 ($^1J_{PtP}$ = 2783 Hz).

All details concerning characterization of **1b**−**1h**, **2b**−**2h**, **3b**−**3h**, and **4b**−**4h** (i.e., synthesis yield, elemental analysis, and ^{1}H/^{31}P NMR) are given in the Supporting Information.

X-ray Data Collection and Structure Determination for 1a and 1f. Light-yellow prismatic crystals of **1a** and (**1f**) suitable for X-ray diffraction were obtained by the slow diffusion of hexane into a concentrated toluene solution and are air-stable. Crystals were mounted on a Bruker SMART diffractometer, equipped with a CCD detector, for the unit cell and space group determination and data collection. Selected experimental crystallographic and other relevant data are listed in Table 8 and in the Supporting Information. Data were corrected for Lorentz and polarization factors with the data reduction software *SAINT*[55] and empirically for absorption using the *SADABS* program.[56] The structures were refined by full-matrix least-squares analysis[57] (with the function minimized being $[\sum w(F_o^2 - (1/k)F_c^2)^2]$). For all structures, no extinction correction was deemed necessary. The scattering factors used, corrected for the real and imaginary parts of the anomalous dispersion, were taken from the literature.[58] All calculations were carried out by using the *WINGX*[59] and *SHELX-97* and *ORTEP*[60] programs.

Structural Study of 1a. The space group was unambiguously determined from the systematic absences, while the cell constants were refined by least squares, at the end of the data collection, using 1024 reflections ($2\theta_{max} \leq 51.83°$). The data were collected by using ω scans, in steps of 0.3°. For each of the 1860 collected frames, the counting time was 30 s.

The Pt atom lies on a crystallographic symmetry element; thus, only half of the molecule is the asymmetric unit. The least-squares refinement was carried out using anisotropic displacement parameters for all non-H atoms. The contribution of the H atoms, in their calculated positions, was included in the refinement using a riding model [C−H = 0.96 Å; B(H) = axB(C$_{bonded}$) Å^2], where a = 1.5 for the H atoms of the methyl groups and a = 1.2 for the others).

Structural Study of 1f. The space group was determined from the systematic absences and the successful refinement, while the cell constants were refined by least squares, at the end of the data collection, using 1024 reflections ($2\theta_{max} \leq 51.92°$). The data were collected by using ω scans, in steps of 0.3°. For each of the 1850 collected frames, the counting time was 40 s.

The least-squares refinement was carried out using anisotropic displacement parameters for all non-H atoms, while the H atoms were included in the refinement as described above. Refining the Flack's parameter[61] tested the handedness of the structure.

Kinetic Measurements. Protonolysis and deuterolysis reactions of **1a**−**1f** were followed by conventional spectrophotometric techniques in methanol and methanol-d_4, respectively, under pseudo-first-order conditions and were started by injecting solutions of HOTf or DOTf to solutions of dibenzyl complexes with acid in excess. The second-order rate constants for protonolysis, k_H, at 297 K were obtained by least-squares regression analysis of the linear plots of the pseudo-first-order rate constants versus the concentration of the acid. At other temperatures, the values of k_H were obtained from the ratio of the measured pseudo-first-order rate constants k_{obsd} to [H$^+$]. The kinetics of isomerization of the solvento complexes **3a**−**3h** in acetonitrile were followed in the UV region by stopped-flow spectrophotometric techniques. Fresh solutions of the complexes (0.05−0.1 mM) were used for all kinetic runs. The reactions were carried out in the thermostatted cell of the instrument, with a temperature accuracy of ±0.02 °C, and were started by injecting acetonitrile solutions of HBF$_4$ into solutions of dibenzyl complexes (in a 100:1 acid-to-complex ratio). The acid concentration does not affect the isomerization reaction and was calculated to produce a very fast cleavage of the Pt−benzyl bond. All reactions obeyed a first-order rate law until well over 90% of the reaction, and the rate constants, k_{obsd}/s^{-1}, were obtained from a nonlinear least-squares fit of the experimental data to $D_t = D_\infty + (D_0 - D_\infty)\exp(-k_{obsd}t)$ with D_0, D_∞, and k_{obsd} as the parameters to be optimized (D_0 = absorbance after mixing of the reagents; D_∞ = absorbance at completion of the reaction). Activation parameters were derived from a linear least-squares analysis of ln(k_{obsd}/T) vs T^{-1} data according to the linear expression of the Eyring equation

$$\ln\left(\frac{k}{T}\right) = \left(\frac{k_B}{h} + \frac{\Delta S^{\ddagger}}{R}\right)\frac{\Delta H^{\ddagger}}{RT} \qquad (5)$$

and are listed in Table 4.

Computational Details. Geometry optimizations as well as frequency calculations for all of the model complexes considered here were performed at the DFT level, employing Becke's three-parameter hybrid functional[62] combined with the Lee, Yang, and Parr (LYP)[63] correlation functional, denoted as B3LYP within the *GAUSSIAN03/DFT* package.[64] The LANL2DZ effective-core potential[65] was used for the metal center. In LANL2DZ, the valence shell is explicitly represented using a double-ζ and includes both n = 5(s,pd) and n = 6(s) orbitals. The standard 6-31+G** basis set[66] was employed for the rest of the atoms.

No symmetry restrictions were imposed during the geometry optimizations, whereas for each optimized stationary point, vibrational analysis was performed to determine its character (minimum or saddle point) and to evaluate the zero-point vibrational energy corrections, which are included in all relative energies. For all of the reported TSs, it was carefully checked that the vibrational mode associated with the imaginary frequency corresponds to the correct movement of involved atoms. All of the minima connected by a given TS were confirmed by intrinsic reaction coordinate[67] driving calculations (in mass-weighted coordinates), as implemented in the *Gaussian03* program.

■ ASSOCIATED CONTENT

Supporting Information. Experimental Section giving ^{1}H/^{31}P{^{1}H} NMR complex characterization, yields, and elemental analysis for the starting complexes **1b**−**1h**, the intermediate species

2b−**2h** and **3b**−**3h**, and the final compounds **4b**−**4d**, tables giving rate constants for protonolysis and deuterolysis of the Pt−C bond on complex **1c** in methanol, temperature dependence of the reductive-elimination rate constants for **3d**, all primary kinetic data for isomerization of **3a**−**3h** in CH_3CN, and Cartesian coordinates of the B3LYP-optimized T-shaped *cis*- and *trans*-$[Pt(CH_2C_6H_4Y)(PMe_3)_2]^+$ (Y = H, 4-Cl, 4-Me) species, figures showing a view of a molecule of compound **1f** with a weak nonconventional Pt···H interaction with H7, exponential curves for molar fraction variation as a function of time and an Eyring plot for the reductive-elimination reaction, a typical kinetic run for the isomerization reaction and for reductive elimination, dependence of the coupling constants $^1J_{PtP}$ for the benzylhydridoplatinum(IV) complexes **2a**−**2h** on Hammett's σ of substituent groups, correlation between the experimental and computed free energies of activation for isomerization, DFT-optimized geometrical structures of the **V** and **VI** $[Pt(CH_2C_6H_5)(MeOH)(PEt_3)_2]^+$, PES plots showing the electronic effects on the activation energy for isomerization of *cis*-$[Pt(CH_2C_6H_4\text{-}4Y)(PEt_3)_2]$ by para-substituent groups on the benzyl rings, and crystallographic data for structures **1a** and **1f** in CIF format. This material is available free of charge via the Internet at http://pubs.acs.org.

AUTHOR INFORMATION

Corresponding Author

*Phone: +39-090-6765734. Fax: +39-090-3974108. E-mail: rosaria.plutino@pa.ismn.cnr.it.

ACKNOWLEDGMENT

We are grateful to the MURST (PRIN 2007), University of Messina (PRA 2004), and CNR for funding this work. E. Guido, G. D'Amico, A. Romeo, and M. R. Plutino wish to thank Mr. G. Irrera for technical assistance.

DEDICATION

†Dedicated to the memory of Professor Raffaello Romeo, who died on February 23, 2009.

REFERENCES

(1) (a) Collman, J. P.; Hegedus, L. S.; Norton, J. R.; Finke, R. C. *Principles and Applications of Organotransition Metal Chemistry*; University Science Books: Mill Valley, CA, 1987. (b) Crabtree, R. H. *The Organometallic Chemistry of the Transition Metals*; Wiley-Interscience: New York, 1994. (c) Yamamoto, A. *Organotransition Metal Chemistry*; Wiley: New York, 1986. (d) James, B. R. In *Comprehensive Organometallic Chemistry*; Wilkinson, G., Stone, F. G. A., Abel, E. W., Eds.; Pergamon Press: Oxford, U.K., 1982; Chapter 51. (e) Parshall, G. W. *Homogeneous Catalysis*; Wiley-Interscience: New York, 1980.

(2) (a) Strauss, S. H. *Chem. Rev.* **1993**, *93*, 927–942. (b) Huang, D.; Huffman, J. C.; Streib, W. E.; Bollinger, J. C.; Eisenstein, O.; Caulton, K. G. *J. Am. Chem. Soc.* **1997**, *119*, 7398–7399. (c) Kulawiec, R. J.; Crabtree, R. H. *Coord. Chem. Rev.* **1990**, *99*, 89–115.

(3) (a) Moncho, S.; Ujaque, G.; Lledos, A.; Espinet, P. *Chem.—Eur. J.* **2008**, *14*, 8986–8994. (b) Casares, J. A.; Espinet, P.; Salas, G. *Chem.—Eur. J.* **2002**, *8*, 4843–4853.

(4) (a) Yared, Y. W.; Miles, S. L.; Bau, R.; Reed, C. A. *J. Am. Chem. Soc.* **1977**, *99*, 7076–7078. (b) Knobler, C. B.; Marder, T. B.; Mizusawa, E. A.; Teller, R. G.; Long, J. A.; Behnken, P. E.; Hawthorne, M. F. *J. Am. Chem. Soc.* **1984**, *106*, 2990–3004. (c) Urtel, H.; Meier, C.; Eisentränger, F.; Rominger, F.; Joschek, J. P.; Hofmann, P. *Angew. Chem., Int. Ed.* **2001**, *40*, 781–784. (d) Chaplin, A. B.; Poblador-Bahamonde, A. I.; Sparkes, H. A.; Howard, J. A. K.; Macgregor, S. A.; Weller, A. S. *Chem. Commun.* **2009**, 244–246. (e) Dias, E. L.; Brookhart, M.; White, P. S. *Chem. Commun.* **2001**, 423–424. (f) Budzelaar, P. H. M.; de Gelder, R.; Gal, A. W. *Organometallics* **1998**, *17*, 4121–4123.

(5) (a) Ingleson, M.; Fan, H. J.; Pink, M.; Tomaszewski, J.; Caulton, K. G. *J. Am. Chem. Soc.* **2006**, *128*, 1804–1805. (b) Ingleson, M. J.; Pink, M.; Caulton, K. G. *J. Am. Chem. Soc.* **2006**, *128*, 4248–4249.

(6) (a) Hay-Motherwell, R.; Wilkinson, G.; Sweet, T. K. N.; Hursthouse, M. B. *Polyhedron* **1996**, *15*, 3163–3166. (b) Mindiola, D. J.; Hillhouse, G. L. *J. Am. Chem. Soc.* **2001**, *123*, 4623–4624.

(7) (a) Stambuli, J. P.; Bühl, M.; Hartwig, J. F. *J. Am. Chem. Soc.* **2002**, *124*, 9346–9347. (b) Stambuli, J. P.; Incarvito, C. D.; Bühl, M.; Hartwig, J. F. *J. Am. Chem. Soc.* **2004**, *126*, 1184–1194. (c) Yamashita, M.; Hartwig, J. F. *J. Am. Chem. Soc.* **2004**, *126*, 5344–5345. (d) Campora, J.; Gutiérrez-Puebla, E.; Lopez, J. A.; Monge, A.; Palma, P.; Del Rio, D.; Carmona, E. *Angew. Chem., Int. Ed.* **2001**, *40*, 3641–3644.

(8) (a) Carr, N.; Mole, L.; Orpen, A. G.; Spencer, J. L. *J. Chem. Soc., Dalton Trans.* **1992**, 2653–2662. (b) Mole, L.; Spencer, J. L.; Carr, N.; Orpen, A. G. *Organometallics* **1991**, *10*, 49–52. (c) Ingleson, M. J.; Mahon, M. F.; Weller, A. S. *Chem. Commun.* **2004**, 2398–2399. (d) Baratta, W.; Stoccoro, S.; Doppiu, A.; Herdtweck, E.; Zucca, A.; Rigo, P. *Angew. Chem., Int. Ed.* **2003**, *42*, 105–109. (e) Braunschweig, H.; Radacki, K.; Rais, D.; Scheschkewitz, D. *Angew. Chem., Int. Ed.* **2005**, *44*, 5651–5654. (f) Braunschweig, H.; Radacki, K.; Uttinger, K. *Chem.—Eur. J.* **2008**, *14*, 7858–7866.

(9) Pregosin, P. S. *Chem. Commun.* **2008**, 4875–4884 and references cited therein.

(10) Scott, N. M.; Dorta, R.; Stevens, E. D.; Correa, A.; Cavallo, L.; Nolan, S. P. *J. Am. Chem. Soc.* **2005**, *127*, 3516–3526.

(11) Romeo, R.; D'Amico, G.; Sicilia, E.; Russo, N.; Rizzato, S. *J. Am. Chem. Soc.* **2007**, *129*, 5744–5755.

(12) (a) Romeo, R. *Comments Inorg. Chem.* **2002**, *23*, 79–100 and references cited therein. (b) Romeo, R.; Plutino, M. R.; Elding, L. I. *Inorg. Chem.* **1997**, *36*, 5909–5916. (c) Romeo, R.; Alibrandi, G. *Inorg. Chem.* **1997**, *36*, 4822–4830. (d) Alibrandi, G.; Minniti, D.; Monsù Scolaro, L.; Romeo, R. *Inorg. Chem.* **1988**, *27*, 318–324. (e) Romeo, R.; Minniti, D.; Lanza, S.; Uguagliati, P.; Belluco, U. *Inorg. Chem.* **1978**, *17*, 2813–2818.

(13) For a discussion on dissociative pathways in platinum(II) chemistry, see: (a) Romeo, R. *Comments Inorg. Chem.* **1990**, *11*, 21–57.

(14) Carmona, E.; Marin, J. M.; Paneque, M.; Poveda, M. L. *Organometallics* **1987**, *6*, 1757–1765 and references cited therein.

(15) Chatt, J.; Shaw, B. L. *J. Chem. Soc.* **1959**, *705*, 4020–4033.

(16) Romeo, R.; D'Amico, G. *Organometallics* **2006**, *25*, 3435–3446.

(17) (a) Allen, F. H.; Pidcock, A. *J. Chem. Soc. A* **1968**, 2700–2704. (b) Appleton, T. G.; Clark, H. C.; Manzer, L. E. *Coord. Chem. Rev.* **1973**, *10*, 335–422.

(18) Rizzato, S.; Bergès, J.; Mason, S. A.; Albinati, A.; Kozelka, J. *Angew. Chem., Int. Ed.* **2010**, *49*, 7440–7443.

(19) The spectra for protonolysis and isomerization, obtained using a very large amount of acid (1 M) to accelerate the first reaction (Pt−C bond breaking) were hardly discernible. A treatment of the kinetic data with the equation for consecutive reactions gave approximate values of rate constants of $k_H = 250\ s^{-1}$ and $k_i = 108\ s^{-1}$, respectively at 298 K. As a result, a proper study of the second fast process (isomerization) is prevented, but it is still possible to perform a systematic study of protonolysis.

(20) Wik, B. J.; Lersh, M.; Tilset, M. *J. Am. Chem. Soc.* **2002**, *124*, 12116–12117.

(21) (a) Appleton, T. G.; Bennett, M. A. *Inorg. Chem.* **1978**, *17*, 738–747. (b) Grim, S. O.; Keiter, R. L.; McFarlane, W. *Inorg. Chem.* **1967**, *6*, 1133–1137. (c) Allen, F. H.; Sze, S. N. *J. Chem. Soc. A* **1971**, 2054–2056.

(22) Pregosin, P. S.; Kunz, R. W. In *^{31}P and ^{13}C NMR of Transition Metal Complexes*; Diehl, P., Fluck, E., Kosfeld, R., Eds.; Springer: New York, 1979.

(23) Garrou, P. E. *Inorg. Chem.* **1975**, *14*, 1435–1439.

(24) (a) Cobley, C. J.; Pringle, P. *Inorg. Chim. Acta* **1997**, *265*, 107–115.(b) Pregosin, P. S. . In *Organic Compounds and Metal Complexes*; Verkade, J. G., Quin, L. D., Eds.; VCH: New York, 1987; Chapter 13 and references cited therein.

(25) (a) Mather, G. G.; Pidcock, A.; Rapsey, G. J. N. *J. Chem. Soc., Dalton Trans.* **1973**, 2095–2099. (b) Crispini, A.; Harrison, K. N.; Orpen, A. G.; Pringle, P. G.; Wheatcroft, J. R. *J. Chem. Soc., Dalton Trans.* **1996**, 1069–1076.

(26) (a) Romeo, R.; Carnabuci, S.; Plutino, M. R.; Romeo, A.; Rizzato, S.; Albinati, A. *Inorg. Chem.* **2005**, *44*, 1248–1262. (b) Romeo, R.; Monsù Scolaro, L.; Plutino, M. R.; Fabrizi de Biani, F.; Bottari, G.; Romeo, A. *Inorg. Chim. Acta* **2003**, *350*, 143–151. (c) Romeo, R.; Plutino, M. R.; Monsù Scolaro, L.; Stoccoro, S. *Inorg. Chim. Acta* **1997**, *265*, 225–233. (d) Romeo, R.; Arena, G.; Monsù Scolaro, L. *Inorg. Chem.* **1994**, *33*, 4029–4037.

(27) (a) Belluco, U.; Giustiniani, M.; Graziani, M. *J. Am. Chem. Soc.* **1967**, *89*, 6494–6500. (b) Romeo, R.; Minniti, D.; Lanza, S.; Uguagliati, P.; Belluco, U. *Inorg. Chem.* **1978**, *17*, 2813–2818. (c) Jawad, J. K.; Puddephatt, R. J. *J. Chem. Soc., Chem. Commun.* **1977**, 892. (d) Romeo, R.; Minniti, D.; Lanza, S. *J. Organomet. Chem.* **1979**, *165*, C36–C38. (e) Jawad, J. K.; Puddephatt, R. J.; Stalteri, M. A. *Inorg. Chem.* **1982**, *21*, 332–337. (f) Alibrandi, G.; Minniti, D.; Monsù Scolaro, L.; Romeo, R. *Inorg. Chem.* **1988**, *27*, 318–324. (g) Yang, D. S.; Bancroft, G. M.; Bozek, J. D.; Puddephatt, R. J.; Tse, J. S. *Inorg. Chem.* **1989**, *28*, 1–2. (h) Yang, D. S.; Bancroft, G. M.; Puddephatt, R. J.; Tan, K. H.; Cutler, J. N.; Bozek, J. D. *Inorg. Chem.* **1990**, *29*, 4956–4960.

(28) (a) Abraham, M. H. In *Comprehensive Chemical Kinetics*; Bamford, C. H., Tipper, C. F. H., Eds.; Elsevier: Amsterdam, The Netherlands, 1973. (b) Eaborn, C. *J. Organomet. Chem.* **1975**, *100*, 43–57. (c) Kochi, J. K. *Organometallic Mechanisms and Catalysis*; Academic Press: New York, 1978; pp 292−340.

(29) (a) Perutz, R. N.; Sabo-Etienne, S. *Angew. Chem., Int. Ed.* **2007**, *46*, 2578–2592. (b) Lersch, M.; Tilset, M. *Chem. Rev.* **2005**, *105*, 2471–2526. (c) Wick, D. D.; Goldberg, K. I. *J. Am. Chem. Soc.* **1997**, 10235–10236. (d) Johansson, L.; Ryan, O. B.; Tilset, M. *J. Am. Chem. Soc.* **1999**, *121*, 1974–1975. (e) Johansson, L.; Tilset, M.; Labinger, J. A.; Bercaw, J. E. *J. Am. Chem. Soc.* **2000**, *122*, 10846–10855. (f) Johansson, L.; Ryan, O. B.; Römming, C.; Tilset, M. *J. Am. Chem. Soc.* **2001**, *123*, 6579–6590. (g) Zhong, H. A.; Labinger, J. A.; Bercaw, J. E. *J. Am. Chem. Soc.* **2002**, *124*, 1378–1399. (h) Labinger, J. A.; Bercaw, J. E. *Nature* **2002**, *417*, 507–514. (i) Heyduck, A. F.; Driveer, T. G.; Day, M. W.; Labinger, J. A.; Bercaw, J. E. *J. Am. Chem. Soc.* **2004**, *126*, 15034–15035. (j) Driver, T. G.; Labinger, J. A.; Bercaw, J. E. *Organometallics* **2005**, *24*, 3644–3654. (k) Williams, T. J.; Labinger, J. A.; Bercaw, J. E. *Organometallics* **2007**, *26*, 281–287. (l) Driver, T. G.; Williams, T. J.; Labinger, J. A.; Bercaw, J. E. *Organometallics* **2007**, *26*, 294–301. (m) Williams, T. J.; Caffyn, A. J. M.; Hazary, N.; Oblad, P. F.; Labinger, J. A.; Bercaw, E. J. *J. Am. Chem. Soc.* **2008**, *130*, 2418–2419.

(30) (a) Romeo, R.; Plutino, M. R.; Romeo, A. *Helv. Chim. Acta* **2005**, *88*, 507–522. (b) Marrone, A.; Re, N.; Romeo, R. *Organometallics* **2008**, *27*, 2215–2222.

(31) (a) De Felice, V.; De Renzi, A.; Panunzi, A.; Tesauro, D. *J. Organomet. Chem.* **1995**, *488*, C13–C14. (b) Hill, G. S.; Rendina, L. M.; Puddephatt, R. J. *Organometallics* **1995**, *14*, 4966–4968. (c) Stahl, S. S.; Labinger, J. A.; Bercaw, J. E. *J. Am. Chem. Soc.* **1995**, *117*, 9371–9372.

(32) (a) O'Reilly, S. A.; White, P. S.; Templeton, J. L. *J. Am. Chem. Soc.* **1996**, *118*, 5684–5689. (b) Canty, A. J.; Dedieu, A.; Jin, H.; Milet, A.; Richmond, M. K. *Organometallics* **1996**, *15*, 2845–2847. (c) Reinartz, S.; White, P. S.; Brookhart, M.; Templeton, J. L. *J. Am. Chem. Soc.* **2001**, *123*, 12724–12725. (d) Reinartz, S.; White, P. S.; Brookhart, M.; Templeton, J. L. *Organometallics* **2001**, *20*, 1709–1712. (e) Norris, C. M.; Reinartz, S.; White, P. S.; Templeton, J. L. *Organometallics* **2002**, *21*, 5649–5656. (f) Hill, G. S.; Puddephatt, R. J. *J. Am. Chem. Soc.* **1996**, *118*, 8745–8746. (g) Hill, G. S.; Vittal, J. J.; Puddephatt, R. J. *Organometallics* **1997**, *16*, 1209–1217. (h) Prokopchuk, E. M.; Puddephatt, R. J. *Organometallics* **2003**, *22*, 787–796. (i) Jenkins, H. A.; Klempner, M. J.; Prokopchuk, E. M.; Puddephatt, R. J. *Inorg. Chim. Acta* **2003**, *352*, 72–78. (j) Prokopchuk, E. M.; Jenkins, H. A.; Puddephatt, R. J. *Organometallics* **1999**, *18*, 2861–2866. (k) Puddephatt, R. J. *Coord. Chem. Rev.* **2001**, *219*−*221*, 157–185. (l) Zhang, F.; Prokopchuk, E. M.; Broczkowski, M. E.; Jennings, M. C.; Puddephatt, R. J. *Organometallics* **2006**, *25*, 1583–1591. (m) Vedernikov, A. N.; Fettinger, J. C.; Mohr, F. *J. Am. Chem. Soc.* **2004**, *126*, 11160–11161. (n) Vedernikov, A. N.; Binfield, S. A.; Zavalij, P. Y.; Khusnutdinova, J. R. *J. Am. Chem. Soc.* **2006**, *128*, 82–83.

(33) Rendina, L. M.; Puddephatt, R. J. *Chem. Rev.* **1997**, *97*, 1735–1754.

(34) Stahl, S. S.; Labinger, J. A.; Bercaw, J. E. *J. Am. Chem. Soc.* **1996**, *118*, 5961–5976.

(35) Crumpton-Bregel, D. M.; Goldberg, K. I. *J. Am. Chem. Soc.* **2003**, *125*, 9442–9456.

(36) Examples of C−H reductive elimination from octahedral platinum(IV): (a) Jenkins, H. A.; Yap, G. P. A.; Puddephatt, R. J. *Organometallics* **1997**, *16*, 1946–1955. (b) Fekl, U.; Zahl, A.; van Eldik, R. *Organometallics* **1999**, *18*, 4156–4164. (c) Bartlett, K. L.; Goldgerg, K. I.; Borden, W. T. *J. Am. Chem. Soc.* **2000**, *122*, 1456–1465. (d) Bartlett, K. L.; Goldgerg, K. I.; Borden, W. T. *Organometallics* **2001**, *20*, 2669–2678. (e) Luedtke, A. T.; Goldberg, K. I. *Inorg. Chem.* **2007**, *46*, 8496–8498. (f) Jensen, M. P.; Wick, D. D.; Reinartz, S.; White, P. S.; Templeton, J. L.; Goldberg, K. I. *J. Am. Chem. Soc.* **2003**, *125*, 8614–8624. (g) Puddephatt, R. J. *Angew. Chem., Int. Ed.* **2002**, *41*, 261–263. (h) Milstein, D. *J. Am. Chem. Soc.* **1982**, *104*, 5227–5228.

(37) (a) Fekl, U.; Kaminsky, W.; Goldberg, K. I. *J. Am. Chem. Soc.* **2001**, *123*, 6423–6424. (b) Reinartz, S.; White, P. S.; Brookhart, M.; Templeton, J. L. *J. Am. Chem. Soc.* **2001**, *123*, 6425–6426.

(38) (a) Lo, H. C.; Haskel, A.; Kapon, M.; Keinan, E. *J. Am. Chem. Soc.* **2002**, *124*, 3226–3228. (b) Jones, W. D. *Acc. Chem. Res.* **2003**, *36*, 140–146.

(39) (a) Lian, T.; Bromberg, S. E.; Yang, H.; Proulz, G.; Bergman, R. G.; Harris, C. B. *J. Am. Chem. Soc.* **1996**, *118*, 3769–3770. (b) Bromberg, S. E.; Yang, H.; Asplund, M. C.; Lian, T.; McNamara, B. K.; Kotz, K. T.; Yeston, J. S.; Wilkens, M.; Frei, H.; Bergman, R. G.; Harris, C. B. *Science* **1997**, *278*, 260–263. (c) Crabtree, R. H. *Chem. Rev.* **1995**, *95*, 987–1007. (d) Hall, C.; Perutz, R. N. *Chem. Rev.* **1996**, *96*, 3125–3146.

(40) (a) Hill, G. S.; Puddephatt, R. J. *Organometallics* **1998**, *17*, 1478–1486. (b) Siegbahn, P. E. M.; Crabtree, R. H. *J. Am. Chem. Soc.* **1996**, *118*, 4442–4450. (c) Bartlett, K. L.; Goldberg, K. I.; Borden, W. T. *J. Am. Chem. Soc.* **2000**, *122*, 1456–1465. (d) Bartlett, K. L.; Goldberg, K. I.; Borden, W. T. *Organometallics* **2001**, *20*, 2669–2678. (e) Heiberg, H.; Johansson, L.; Gropen, O.; Ryan, O. B.; Swang, O.; Tilset, M. *J. Am. Chem. Soc.* **2000**, *122*, 10831–10845. (f) Gilbert, T. M.; Hristov, I.; Ziegler, T. *Organometallics* **2001**, *20*, 1183–1189.

(41) Johansson, L.; Tilset, M. *J. Am. Chem. Soc.* **2001**, *123*, 739–740.

(42) Plutino, M. R.; Monsù Scolaro, L.; Albinati, A.; Romeo, R. *J. Am. Chem. Soc.* **2004**, *126*, 6470–6484.

(43) Iodide dissociation that precedes ethane elimination from $[PdIMe_3(bpy)]$ is characterized by a very large negative entropy of activation ($\Delta S^{\ddagger} = -53 \pm 25$ and -164 ± 17 J K^{-1} mol^{-1}) in acetone and methanol, respectively. Byers, P. K.; Canty, A. J.; Crespo, M.; Puddephatt, R. J.; Scott, J. D. *Organometallics* **1988**, *7*, 1363–1367.

(44) Preliminary results of a kinetic study of solvent exchange between free and coordinated acetonitrile in $[Pt(dppe)(CH_3)(CH_3CN]^+$ by ^{1}H NMR magnetization transfer experiments have shown that the exchange is very fast ("rate" = k_2[Complex][CH_3CN], with $k_2 = 0.711$ s^{-1} at 298 K in CD_2Cl_4). The exchange takes place with an associative mode of activation. The presence of a similar process on *cis*-$[Pt(PEt_3)_2(CH_2R)(CH_3CN)]^+$ is obvious, but it is fruitless in affecting isomerization. Rather, the exchange gives an independent clear-cut indication that the rate of reentry of CH_3CN on *cis*-$[Pt(PEt_3)_2(CH_2R)]^+$ must be very high and that the condition ($k_{-D} \gg k_T$) for a preequilibrium treatment in deriving the rate law is totally fulfilled.

(45) As an example, the complex *cis*-$[Pt(PEt_3)_2(Me)_2]$ does not isomerize. The complex *cis*-$[Pt(PEt_3)_2(Me)Cl]$ is stable in dichloromethane and in a number of nonpolar solvent. Its rate of isomerization increases upon an increase in the electrophilic character of the solvent, which is important in promoting Pt−Cl bond breaking (Romeo, R.; Minniti, D.; Lanza, S. *Inorg. Chem.* **1980**, *19*, 3663–3668). The rate of isomerization of the cationic solvento complexes *cis*-$[Pt(PEt_3)_2(Me)(S)]^+$ depends on the coordinating properties of the solvent being very low when S is acetonitrile ($t_{1/2} \approx 24$ h[11]),

much higher in methanol ($t_{1/2} \approx 6$ min[12b]), and instantaneous in noncoordinating solvents..

(46) (a) Thorn, D. L.; Hoffmann, R. *J. Am. Chem. Soc.* **1978**, *100*, 2079–2090. (b) McCarthy, T. J.; Nuzzo, R. G.; Whitesides, G. M. *J. Am. Chem. Soc.* **1981**, *103*, 3396–3403. (c) Tatsumi, K.; Hoffmann, R.; Yamamoto, A.; Stille, J. K. *Bull. Chem. Soc. Jpn.* **1981**, *54*, 1857–1867.

(47) (a) Crascall, L. E.; Lister, S. A.; Redhouse, A. D.; Spencer, J. L. *J. Organomet. Chem.* **1990**, *394*, C35–C38. (b) Zhao, S.; Wu, G.; Wang, S. *Organometallics* **2006**, *25*, 5979–5989. (c) Sonoda, A.; Bailey, P. M.; Maitlis, M. *J. Chem. Soc., Dalton Trans.* **1979**, 346–350. (d) Rix, F. C.; Brookart, M.; White, P. S. *J. Am. Chem. Soc.* **1996**, *118*, 2436–2448. (e) Gatti, G.; Lopez, J. A.; Mealli, C.; Musco, A. *J. Organomet. Chem.* **1994**, *483*, 77–89. (f) Carmona, E.; Marin, J. M.; Paneque, M.; Poveda, M. L. *Organometallics* **1987**, *6*, 1757–1765. (g) Albers, I.; Alvarez, E.; Càmpora, J.; Maya, C. M.; Palma, P.; Sànchez, L. J.; Passaglia, E. *J. Organomet. Chem.* **2004**, *689*, 833–839. (h) Nettekoven, U.; Hartwig, F. *J. Am. Chem. Soc.* **2002**, *124*, 1166–1167. (i) Komon, Z. J. A.; Bu, X.; Bazan, G. C. *J. Am. Chem. Soc.* **2000**, *122*, 12379–12380.

(48) Konze, W. V.; Scott, B. L.; Kubas, G. J. *J. Am. Chem. Soc.* **2002**, *124*, 12550–12556.

(49) (a) Driver, T. G.; Day, M. W.; Labinger, J. A.; Bercaw, J. E. *Organometallics* **2005**, *24*, 3644–3654. (b) Driver, T. G.; Travis, J. W.; Labinger, J. A.; Bercaw, J. E. *Organometallics* **2007**, *25*, 294–301.

(50) As the Pt−O distance increases, the absolute energy of the complex likewise increases until the MeOH molecule is far enough for the onset of interaction of the *ipso*-C atom of the benzyl ligand with the metal atom (structure **Σ** in Figure S7 in the Supporting Information). As a consequence, the absolute energy of the system decreases and tends to the asymptotic limit represented by the sum of the separated T-shaped complex and solvent molecule energies (structure **Ω**). The stabilization energy was calculated as the energy difference between the **Σ** and **Ω** structures.

(51) Riddick, J. A.; Bunger, W. B.; Sakano, T. K. In *Organic Solvents*, 4th ed.; Weissberger, A., Ed.; John Wiley & Sons: New York, 1986.

(52) Brookhart, M.; Grant, B.; Volpe, J. *Organometallics* **1992**, *11*, 3920–3922.

(53) (a) Van Geet, A. L. *Anal. Chem.* **1968**, *40*, 2227–2229. (b) Van Geet, A. L. *Anal. Chem.* **1970**, *42*, 679–680.

(54) Applied Photophysics Bio Sequential SX-17 MV, sequential stopped-flow ASVD spectrofluorimeter: *Software Manual*; Applied Photophysics Ltd.: Leatherhead, U.K., 1993.

(55) BrukerAXS. *SAINT, Integration Software*; Bruker Analytical X-ray Systems: Madison, WI, 1995.

(56) Sheldrick, G. M. *SADABS, Program for Absorption Correction*; University of Göttingen: Göttingen, Germany, 1996.

(57) Sheldrick, G. M. *Acta . Crystallogr.* **2008**, *A64*, 112–122.

(58) *International Tables for X-ray Crystallography*; Wilson, A. J. C., Ed.; Kluwer Academic Publisher: Dordrecht, The Netherlands, 1992; Vol. C.

(59) Farrugia, L. J. *J. Appl. Crystallogr.* **1999**, *32*, 837–838.

(60) Farrugia, L. J. *J. Appl. Crystallogr.* **1997**, *30*, 565–566.

(61) Flack, H. D. *Acta Crystallogr.* **1983**, *A39*, 876–881.

(62) Becke, A. D. *J. Chem. Phys.* **1993**, *98*, 5648–5652.

(63) Stephens, P. J.; Devlin, F. J.; Chabalowski, C. F.; Frisch, M. J. *J. Phys. Chem.* **1994**, *98*, 11623–11627.

(64) Frisch, M. J. et al. *Gaussian03*, revision A.1; Gaussian, Inc.: Pittsburgh, PA, 2003.

(65) (a) Hay, P. J.; Wadt, W. R. *J. Chem. Phys.* **1985**, *82*, 270–283. (b) Wadt, W. R.; Hay, P. J. *J. Chem. Phys.* **1985**, *82*, 284–298. (c) Hay, P. J.; Wadt, W. R. *J. Chem. Phys.* **1985**, *82*, 299–310.

(66) (a) Krishnan, R.; Binkley, J. S.; Seeger, R.; Pople, J. A. *J. Chem. Phys.* **1980**, *72*, 650–654. (b) Blaudeau, J. P.; McGrath, M. P.; Curtiss, L. A.; Radom, L. *J. Chem. Phys.* **1997**, *107*, 5016–5021.

(67) (a) Gonzalez, C.; Schlegel, H. B. *J. Chem. Phys.* **1989**, *90*, 2154–2161. (b) Gonzalez, C.; Schlegel, H. B. *J. Phys. Chem.* **1990**, *94*, 5523–5527.